A Metallurgical Investigation of the Effects of Double Tempering on the Hardness, Impact Toughness and Microstructure of AISI 4140 Steel

A Major Qualifying Project Submitted to
the Faculty of Worcester Polytechnic Institute
in partial fulfillment of the requirements for the
Degree in Bachelor of Science in Mechanical Engineering

By

Aidan Freeburg

Connor Hoeckele

Connor Ross

Kelly Soto

Date: 4/26/18

Project Advisors:

Professor Richard Sisson

Abstract

Low alloy steels are commonly used in industry for a wide range of applications that require high strength and toughness. Each application requires specific properties. In order to modify the alloy's properties to meet these specifications, a variety of heat treatment techniques are employed, including annealing, quenching, and tempering. Tempering is a metallurgical process by which toughness and ductility are improved. This procedure is conducted by heating the as-quenched martensitic steel to temperatures in the ferrite plus cementite phase region for several hours. Tempering is generally carried out in a single cycle temperature-time. However, the procedure may be conducted in two cycles with cooling to room temperature between the cycles. This process is known as double tempering. The goal of this project is to investigate the effects of single versus double tempering on the mechanical properties and microstructure of 4140 steel. To achieve this goal, samples of 4140 steel were quenched and tempered at 300, 400, 500, and 600 ºC for the same total heat time in single and double tempers. The samples were machined to ASTM standard impact testing. The Rockwell hardness and Charpy V-notch impact energy were measured. The microstructure was characterized using optical and scanning electron microscopy (SEM), and carbides were extracted from each sample and XRD was used to determine their size and geometry. The results are analyzed using the Holloman – Jaffe parameter.

It was found that a four-hour double tempering cycle does not significantly alter the microstructure, hardness, or impact toughness of 4140 steel when compared to a four hour single tempering cycle.

Acknowledgements

Our Major Qualifying Project team would like to thank all of the individuals and corporations who helped complete the goal of this project. Our team would especially like to thank our advisor Richard Sisson for guiding us through the completion of this project. We would also like to thank Mei Yang, Jin Guo, Haixuan Yu, Xiaoqing Cai, Rita Shilansky, Professor Leebo, and GlorieAnn Minnich for their individual time and assistance in achieving the goal of this project. Our team would also like to extend our gratitude to Thomas Kouttron and, Ian Anderson for their assistance in machining the steel samples to final ASTM standards. Lastly, we would like to thank the following corporations, Bodycote, Peterson Steel Corporation., and Dosco Sheet Metal for helping our team to heat treat and rough cut the 4140 steel samples.

Table of Contents

List of Figures

List of Tables

Introduction

Steel has long been one of the most sought-after materials in the world. One aspect of steel's allure is its ability to be adjusted and manipulated to achieve optimum performance for different applications. Scientists and engineers continue to study how to predict and control the properties of steel by modifying the chemical composition and manufacturing processes of different steel alloys.

AISI 4140 Chromium-molybdenum steel is commonly called 4140 Steel in industry. 4140 Steel is composed of (in weight percentage) 0.38-0.43% Carbon (C), 0.75-1.00% Manganese (Mn), 0.035%(max) Phosphorus (P), 0.04%(max) Sulfur (S), 0.15-0.30% Silicon (Si), 0.80-1.10% Chromium (Cr), 0.15-0.25% Molybdenum (Mo), and the base metal Iron (Fe). The crystal structure of 4140 steel varies between body centered cubic and face centered cubic with varying temperatures and phases. Steel's varying cubic structures allows steel to possess numerous desirable mechanical properties in its solid state.

Based on the composition and mechanical properties that 4140 steel possesses, a wide range of applications in industry can be found. Throughout several heat-treating processes the composition of this material can be altered and lead to other mechanical properties. By manipulating properties such as ductility and machinability, the effectiveness in production of certain parts can be improved. Thus, for its adaptable mechanical properties, 4140 steel is widely desirable among industries. Among these applications, the manufacturing of machinery parts and components are often built using this high carbon grade steel. For example, 4140 is used in common hardware store items such as chain links, nuts and bolts, studs, crowbars, sockets, and tool holders. It is also used in mechanical/machinery applications, with items such as piston rods, gears and cams, pinions, crankshafts, and various machinery parts and components. Due to high desirability and application, 4140 steel was chosen for this study.

To achieve these desire properties after raw product of steel, the steel can undergo a number of different heat treatments. During hardening, steel is heated until it transitions to gamma-phase iron, or austenite, which has a face-centered cubic structure (ASM Handbook, Volume 4A 2013). In this configuration, the steel is capable of dissolving a large amount of carbon; the open nature of the crystalline structure allows for the complete dissolution of carbon. When the workpiece is rapidly cooled, or quenched, it takes on a body-centered tetragonal structure. Because the material is cooled so quickly, the carbon atoms do not have time to diffuse out of the crystal lattice and the result is a very hard, non-equilibrium, highly strained, and carbon supersaturated phase called martensite. The high number of internal dislocations created during the diffusionless austenite-martensite phase transformation is what gives martensite its high hardness, however an as-quenched workpiece will also be very brittle, to the point where it may shatter when dropped (ASM Handbook 2013). In order to increase the toughness of the piece, it must be tempered.

Tempering steel involves heating a quenched workpiece to a specific elevated temperature that is lower than the austenite transformation temperature for a specific amount of time, then allowing it to cool slowly. At this temperature, the martensitic steel will partially decompose into the ferrite and cementite which are the equilibrium phases in the steel. The goal is to retain as much of the strength of martensite as possible while increasing toughness enough to make the piece useable for its given application. For some applications, e.g. the nozzle on a sand blasting machine, a higher hardness is desirable, while on others, e.g. a hammer head, it is important to achieve a high degree of toughness.

Double-tempered pieces are heated, held, and cooled twice. This may have an effect on the mechanical properties of the steel, particularly the impact strength. Double tempering is also used as a selling point for steel-based consumer products; mattress manufacturers advertise the fact that their springs are double-tempered, which they claim will give their mattress a longer usable life. In this project we will study the effects of double-tempering cycles on AISI 4XXX steels, with a focus on AISI 4140.

Currently in industry, companies use different number of tempering cycles depending upon the application and materials of the part being heat treated. One tempering cycle is sufficient for lower alloyed tool steels such as Wl and 01, highly alloyed grades such as H13, S7, A2, D2, and the high-speed steels require multiple tempering cycles. The number of tempering cycles used is also determined by the method in which the piece has been quenched. Liquid quenched steels may be tempered once, air hardened steel require a double temper, and high-speed steels can require a triple temper cycle. Between tempering cycles piece must be cooled, these cooling temperatures vary with number of cycles being used, the temperatures achieved during the tempering cycle, and the cooling method used.

The goal of this project is to investigate if there is a difference in the mechanical properties of steel after a single long tempering cycle and breaking the long cycle up into two tempering cycles.

Background

Before determining if double tempering can make a difference in the mechanical properties of 4140 steel, one must understand the microstructure of steel, how heat treatments affect the microstructure and mechanical properties, and the science behind how those properties are quantified.

4140 steel begins it life in the liquid phase, this phase is the called the austenite phase. Liquid steel is then poured into a cast, where it is cooled down slightly to form a block or cylinder of austenite. These are rough forms from which the final desired products and shapes can be derived from. As the austenite cools it decomposes into ferrite and cementite by the eutectoid reaction, the product phases are arranged in a very characteristic pearlite pattern; the cementite is in the form of plates in a matrix of ferrite.

There are several heat treatment techniques that can be conducted on steel after it has cooled to a ferrite microstructure state and has been cold worked to a near final form. A commonly used heat treatment before the final shaping of steel is annealing. Annealing increases the ductility of the metal, reduces the yield and tensile strength, and reduces the overall hardness of the steel. Annealing is action of heating the cooled steel up to a specific temperature, these temperatures are known and correspond with the various types of steels that are produced.

During annealing the steel microstructure experiences a recrystallization. Recrystallization is the growth of new grains form in a cold-worked metal. These new grains have a greatly reduced number of dislocations compared to the cold-worked metal. With continued time at the annealing temperature, some of the newly formed grains grow at the expense of neighboring grains. There is some further decrease in strength and increase in ductility as the average grain size increases during the grain growth phase of the annealing process. The final grain size depends on the annealing temperature and annealing time. For a particular annealing temperature, as the time at the temperature increases the grain size increases. For a particular annealing time, as the temperature increases the grain size increases. A piece of metal with large grains has lower strength and more ductility than a piece of metal of the same alloy with smaller grains.

Annealed steel is very soft and easy to machine, manufactures will form annealed steel into it desired final form before continue with heat treatments. To increase the hardness of formed steel, the steel will be quenched. In quenching, steel is heated until it forms gamma-phase iron, or austenite, which has a face-centered cubic configuration. Due to this structure, austenite is capable of dissolving a large amount of carbon; the open nature of the structure allows it to absorb carbon from iron carbides in carbon steel. When the workpiece is rapidly cooled, or quenched, it takes on a body-centered tetragonal structure. Because the material is cooled so quickly, the carbon atoms do not have time to diffuse out of the crystal lattice, leading to the development of internal stresses. The result is a microstructure that consists of plates or laths of martensite which is

supersaturated with carbon, which in non-equilibrium, highly strained, In the vast majority of steels, the martensite contains a substantial density of dislocations which are generated during the imperfect accommodation of the shape change accompanying the transformation. The plates may be separated by thin films of retained austenite, the amount of untransformed austenite becoming larger as the martensite-start temperature M_S is reduced.

Upon the completion of quenching, many pieces are tempered to achieve a desired combination of combination of hardness, strength and toughness or to relieve the brittleness of fully hardened steels. The heating of martensite allows the reversal of the unstable crystalline lattice to the stable body centered cubic lattice, produces internal adjustments that relieve stresses and also gives rise to precipitation of carbon particles to grow within the martensite in accordance with temperature and time. The changes during the tempering of martensite can be categorized into stages.

The first tempering stage occurs when iron carbide of epsilon type precipitate with Fe2–3C formula and hexagonal lattice; this carbide may be absent in low-carbon steels and low-alloy steels. The Rockwell hardness of the steel begins to fall, reaching approximately 60 HRC. The second tempering stage occurs when retained austenite in the martensite structure transforms into bainite (in carbon steel). The Rockwell Hardness of the steel continues to fall below 60 HRC

In the third tempering stage, metastable carbide, Fe_5C_2, also known as ferrite and cementite form within the martensite. When this transformation occurs in high-carbon steel, a dark microscopically visible structure is observed in the microstructure. The Rockwell Hardness of the steel is now slightly greater than 50 HRC. The fourth tempering stage take place between 500 °C and 600 °C, and only in steels containing Cr, Mo, V, Nb, or W. In this stage there is precipitation of alloying carbides and the transformation is called ‘secondary hardness.’

Hardness testing

The surface hardness of a material is the resistance of a material to permanent and plastic deformation. Indentation surface hardness testing is the most common method used to determine the hardness of a material. While other forms of hardness testing, such as rebound, electromagnetic, and ultrasonic, are used in a variety of applications and measure material hardness through other techniques, indentation hardness testing provides reliable, and commonly used data. Indentation testing produces quick results and its general use on metals and alloys. Knoop and Vickers testing are suitable for thin materials, coatings, and mounted metallographic components. Brinell testing is used in materials such as cast iron, large steel framework and aluminum.

Indentation hardness testing is measured by loading an indenter of a specified geometry and properties onto the material for a specified length of time and measuring either the depth of penetration or dimensions of the

resulting indentation or impression. As the material being tested is softer, the depth of penetration, or indent dimensions become larger. The Rockwell hardness of the material is calculated is based on an inverse relationship to the measurement of the depth to which an indenter is forced by a heavy total (major) load beyond the depth resulting from a previously applied preliminary (minor) load. Initially a minor load is applied, and a zero-datum position is established. The major load is then applied for a specified period and removed, leaving the minor load applied. The resulting Rockwell number represents the difference in depth from the zero-datum position as a result of the application of the major load. The entire procedure requires as little as a few seconds.

The most common indenter type is a diamond cone ground at 120 degrees for testing hardened steels and carbides. Softer materials are typically tested using tungsten carbide balls ranging in diameters from 1/16" up to 1/2". The combination of indenter and test force make up the Rockwell scale. These combinations make up 30 different scales and are expressed as the actual hardness number followed by the letters HR and then the respective scale. A recorded hardness number of HRC 63 signifies a hardness of 63 on the Rockwell C scale. Higher values indicate harder materials such as hardened steel or tungsten carbide. These can have HRC values in excess of 70 HRC. Rockwell test forces can be applied by either closed loop load cell or traditional deadweight systems.

Impact Testing

Since the early 1820's, scientists and engineers have been publishing research on the effects of impact resistance in metals. In order to accurately and consistently test metals' resistance to dynamic loads, researchers from around the world debated and collaborated for nearly a century to develop a standard impact test. By the 1912 meeting of the American Society for Testing and Materials (ASTM), several pendulum-type machines (very similar to modern designs) had been developed. However, one of the most popular designs was proposed by Georges Charpy of France, and many then adopted "the Charpy test" for their impact testing (Siewert, et al. 1999.)

Modern Charpy impact machines are relatively straightforward and simple to use. As shown in Figure 1, a standard notched specimen is placed between two anvils and a weighted pendulum/hammer is released from a set height to strike and break the sample. When the hammer strikes the notched specimen, a portion of the pendulum's kinetic energy is used to break the sample. The amount of energy used to break the sample is read by the scale and displayed on a computer. This energy is shown as the energy required to break the sample.

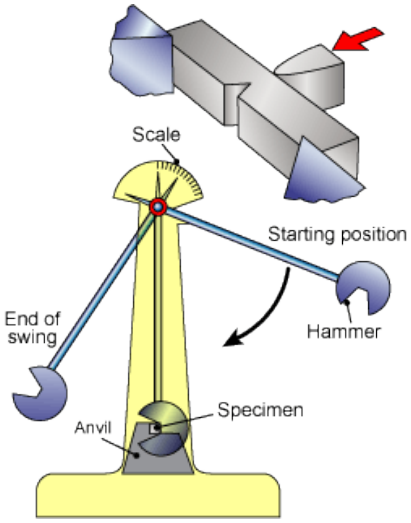

Figure 1: Charpy Impact Test

Hardness, strength, and ductility all play major roles in the impact toughness of metals. Conducting specific tests will be essential in accurately measuring the impact toughness and these other properties of the 4140 steel samples. One of these tests will be the Charpy impact test. Charpy impact testing is very common in the materials science industry and is straightforward to conduct. Samples will be tempered before they are cut down to the standard dimensions for Charpy impact testing. The samples will be made to follow the ASTM Standards for V-Notch Charpy impact testing as shown in Figure 2. Each specimen will cut down from ½" plate stock to 10 mm wide and square and 55 mm in length using water jet cutting. Each sample will be machined to have a notch at the midpoint along one of the 55 mm long faces. These notches will be 2 mm deep going across the 10 mm width of one of the 55 mm long faces on each sample. Each notch will have 0.25 mm radius and the two sides of each notch will create a 45-degree angle.

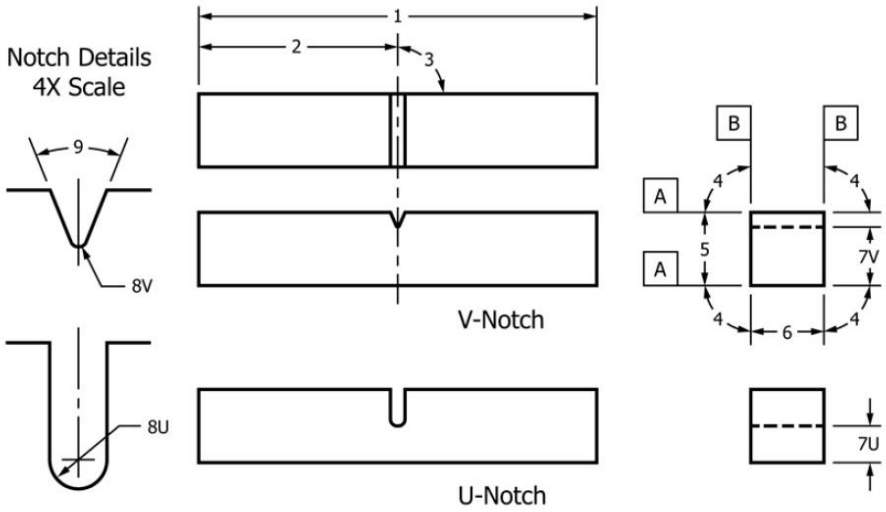

ID Number	Description	Dimension	Tolerance
1	Length of specimen	55 mm	+0/-2.5 mm
2	Centering of notch		±1 mm
3	Notch length to edge	90°	±2°
4	Adjacent sides angle	90°	±0.17°
5	Width	10 mm	±0.075 mm
6	Thickness	10 mm	±0.075 mm
7V	Ligament length, Type V	8 mm	±0.025 mm
7U	Ligament length, Type U	5 mm	±0.075 mm
8V	Radius of notch, Type V	0.25 mm	±0.025 mm
8U	Radius of notch, Type U	1 mm	±0.025 mm
9	Angle of notch	45°	±1°
A	Surface finish requirements	2 μm (Ra)	≤
B	Surface finish requirements	4 μm (Ra)	≤

FIG. 1 Charpy (Simple-Beam) Impact Test Specimens, V-Notch and U-Notch

Figure 2: ASTM Standards for Charpy Impact Test

X-Ray Diffraction

XRD is a nondestructive testing technique used to determine the structure of a crystalline material, in this case Fe carbides such as Cementite (Fe_3C), via the measurement and study of the scattering of incident x-rays as they pass through the crystal and interfere with one another. The pattern in which the x-rays are scattered is dependent on the spacing, structure, and orientation of the crystal lattice, which is distinct for each material. XRD analysis makes it possible to determine the average size and approximate composition of carbides extracted from steel, which gives insight into the microstructure and carbide development for varying temper conditions.

Scanning Electron Microscopy

Scanning Electron Microscopy (SEM) uses a concentrated beam of electrons to examine the microstructure and topography of a sample, typically at a higher magnification than what is possible through optical analysis. The electrons carry a considerable amount of kinetic energy, which is dissipated upon

interaction with the surface of a sample in varying ways. This generates a signal that reveals characteristics of the surface of the material. Study of the fracture surface topography of destructively-tested samples is helpful to determine the mode of failure; examination of polished and etched samples reveals and identifies carbides, grain development, and phases within the steel.

Experimental Plan

This section describes the initial plan discussed to determine if double tempering 4140 steel will produce different mechanical properties than single tempered 4140 steel

To complete this project two 1’ x 1’ x ½” 4140 steel plates will be acquired from Peterson Steel. The direction the plate was rolled in needs to be determined, this is to ensure that the direction the impact testing is not completed in the direction in which the grains were rolled. If the rolling direction is not known the steel samples could be tested in the weakest direction and mechanical property side of 4140 steel. Impact testing must be complete in the direction that is perpendicular to the direction in which the grains are running. Once the direction of the plate is determined the rough sample size can be cut.

A single 1’ x 1’ plate will be selected to be water jet, due to the possibility that an error occurs while cutting. Additionally, an estimate of one hundred samples would be needed for testing, and a single plate will produce an estimated 120 samples. Each sample will be waterjet cut from the ½” plate stock, with the dimensions of 10 mm x 12.7mmx 55mm. The water jet cutting will be completed by Dosco Sheet Metal & Manufacturing Inc, located in Millbury, Massachusetts. The samples will require final milling to the ASTM standards.

Before milling the samples to final dimensions, the samples will need to be quenched. Quenching will be completed by Bodycote Thermal Processing located in Worcester, Massachusetts. Once quenched the Rockwell Hardness of the steel samples will be too hard to be able to safely and affordably mill down the samples to final ASTM standards.

To lower the hardness of samples, the samples will be tempered. Once tempered, the samples will be milled to final dimensions within ASTM standards, the notches will then be cut once the samples have been milled to final dimensions.

For each tempering temperature and time there will be ten samples, divided into two groups. The tempering temperatures that will be used for this experiment are 300, 400, 500, 600 degrees Celsius. At each tempering temperature, one group will be tempered for four straight hours, the second group will have the four

hours of temper time split into two two hour temper periods. After the first two hours the second group of samples will be removed from the furnace and allowed to air cool to room temperature. The two groups of samples will not be tempered at the same time.

Hardness testing will be completed at the end of the tempering of each sample group. The two two hour tempering group will be hardness tested twice. The first test will be completed after the samples have been completely cooled to air temperature after the first two-hour temper. The second testing will be completed after the second two-hour temper. The four-hour temper groups will have hardness testing completed after they have cooled to room temperature.

The 55 mm length and 10 mm width will be measured with calipers to confirm the accuracy of the waterjet cuts, before the samples are machined down from the original .5 inch (12.7mm) height of the source plate to a final height of 10 mm per ASTM specifications. After each piece is machined, its dimensions will be confirmed to be within the ASTM specification using a micrometer.

Once tempered, milled, the notches will be cut with a v-notch broach and the samples will be ready for Charpy Impact Testing. Each sample will be tested individually, the energy absorbed by each sample will be recorded and the fracture surface of each sample will be investigated. The fracture surface of each sample will be examined using SEM (Scanning Electron Microscope). The fracture surface for one side of each sample will be pictured and the fracture surfaces will be compared. A portion of each sample will be cut and finished for carbide extraction.

The carbides will be extracted from the samples using an electro polishing machine. This iterative process entails cutting a small portion of the sample before placing it into the machine. Also, it involves a centrifuge and purification method in which the carbides can be separated from the liquid solution and impurities can be removed respectively. As a final step, the carbides will be prepared for XRD testing by placing them on glass slides.

X-Ray Diffraction (XRD) will be used to determine the size of carbides from each sample. XRD identifies compounds based on their diffraction patterns (size and shape). XRD results from each sample were observed and recorded. Next, the samples were placed under a Scanning Electron Microscope (SEM) to reveal external morphology, crystalline structure, and orientation of materials.

An additional section of the samples will be cut for microstructure analysis of each sample. The cross sections will be mounted with conductive powder and polished up to one micron. The mounted and polished samples will be examined and pictured at 500, 1,000, 5,000, 15,000, and 30,000 magnifications. The external morphology, crystalline structure, and orientation of martensite and carbides will be compared between all the samples.

The results from each test described above will be analyzed for the two tempering methods, and a final conclusion will be made.

Experimental Procedure

This section described the exact procedure completed to achieve the goal of this project and is different than the original plan.

A single one foot by one foot 4140 steel plate was sent to Dosco Sheet Metal to obtain one hundred and twenty-one samples with the dimensions of 10 mm x 12.7mmx 55mm. The direction in which the plate was rolled, was marked with a sharpie permanent marker for the water jet technician. Measuring in the direction in which the plate was rolled, cuts were made every 55mm, in the perpendicular direction cuts were made every 10 mm. A film of coolant was left on the samples upon the completion of water jet cutting.

The rough dimensioned samples were then taken to Bodycote Thermal Processing for quenching. The samples were heated to 850 ºC and quenched in oil. While the samples were completing quenching at Bodycote the furnaced that was used for tempering need to be heat map and location for the samples to be tempered in determined.

The furnace's heat profile was mapped to ensure the consistent heating of samples. A thermocouple was calibrated using ice water and room temperature water to assure correct temperature readings. The thermocouple was then inserted through the top of the furnace, the thermocouple was wired to a National Instruments data acquisition (DAQ) box and the digital reading of the temperature of the furnace was recorded in Celsius. The furnace was mapped in five positions, which can be seen below in Figure 3.

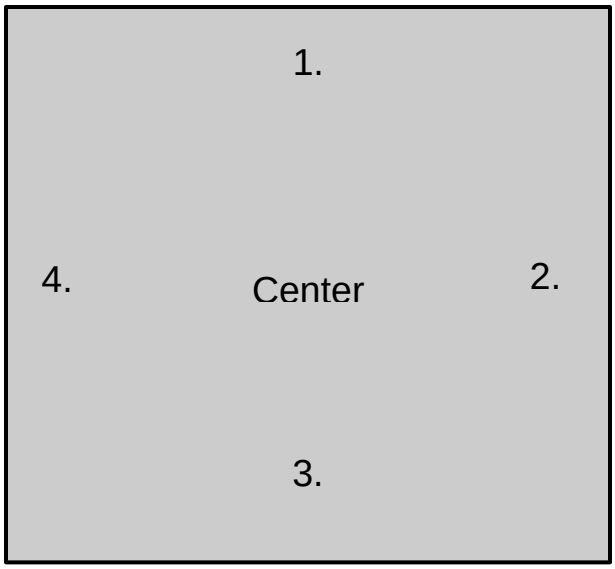

Figure 3: Heat Map Positions

At each position the temperature of the furnace was set on a range of 350 to 550 degrees Celsius in 50 degree increments. The temperature reading was taken from the DAQ box after the temperature on the thermocouple stayed constant for more than one minute. The data collect from each point and each trial can be seen below.

Center			
Trial	Temperature on Dial	Temperature Read on Thermocouple	Variation
	353	361.9	-8.9
	402	412.3	-10.3
	453	470.3	-17.3
	505	521.7	-16.7
	552	570.3	-18.3
		Average Variation-C	-14.3

Table 1: Center Position Temperatures

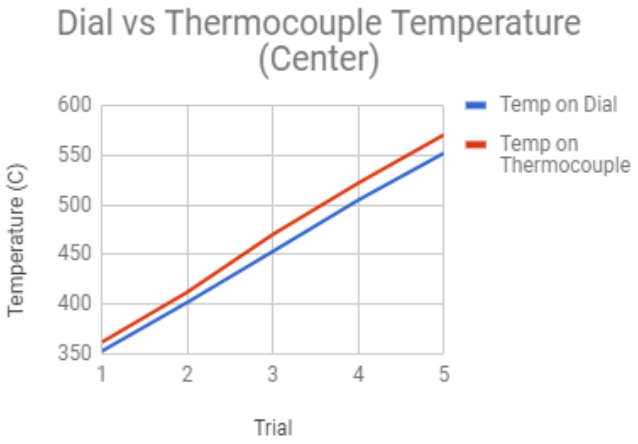

Figure 4: Center Position Dial vs. Thermocouple Temperatures

Location 1 (North)			
Trial	Temperature on Dial	Temperature Read on Thermocouple	Variation
1	350	334.3	15.7
2	402	407.2	-5.2
3	453	457.2	-4.2
4	500	507.7	-7.7
5	554	561.8	-7.8
		Average Variation-C	-1.84

Table 2: Position 1 Temperatures

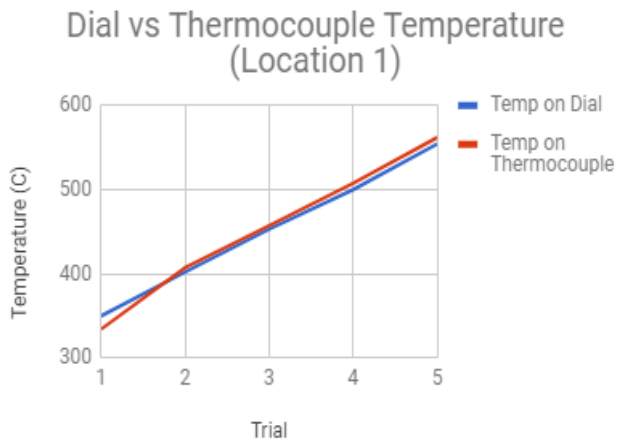

Figure 5: Position 1, Dial vs. Thermocouple Temperatures

Location 2 (East)			
Trial	Temperature on Dial	Temperature Read on Thermocouple	Variation
1	350	349.4	0.6
2	400	402.8	-2.8
3	453	458.6	-5.6
4	505	511.7	-6.7
5	550	563.2	-13.2
		Average Variation-C	-5.54

Table 3: Position 2 Temperatures

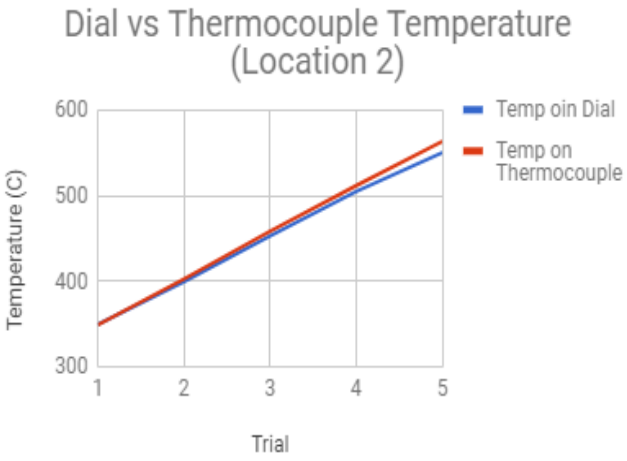

Figure 6: Position 2, Dial vs Thermocouple Temperatures

Location 3 (South)			
Trial	Temperature on Dial	Temperature Read on Thermocouple	Variation
1	350	340.4	9.6
2	402	393.5	8.5
3	453	442.4	10.6
4	500	503.1	-3.1
5	552	555.1	-3.1
		Average Variation-	4.5

Table 4: Position 3 Temperatures

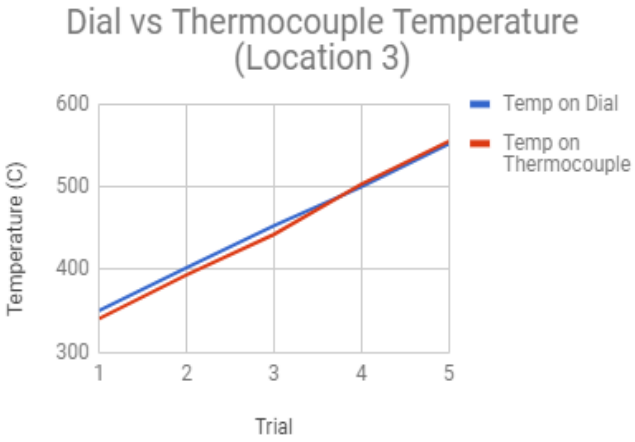

Figure 7: Position 3, Dial vs Thermocouple Temperatures

Location 4 (West)			
Trial	Temperature on in Dial	Temperature Read on Thermocouple	Variation
1	352	353.8	-1.8
2	400	402.6	-2.6
3	453	461.5	-8.5
4	502	513.8	-11.8
5	552	566.7	-14.7
		Average Variation-C	-7.88

Table 5: Position 4 Temperatures

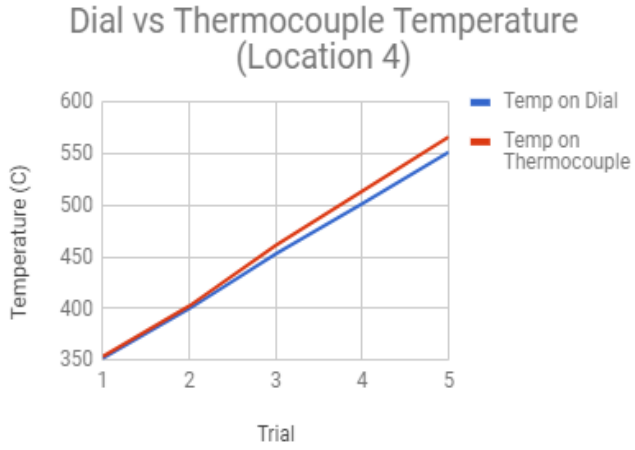

Figure 8: Position 4, Dial vs Thermocouple Temperatures

Analysis of the furnace mapping data suggested that for consistent tempering, the samples should be positioned as close to the center of the furnace as possible. The center of the furnace showed the most variance between the dial reading and the thermocouple reading. The thermocouple was decided to be the controlling temperature reading device during tempering. Tempering temperatures were set to the thermocouple digital reading and not to readout of the furnace.

The samples were then received as-quenched from Bodycote and were ready to be tempered. Tempering temperatures of 300, 400, 500, and 600 degrees Celsius were then selected. For each temperature, one set of five samples was tempered for each tempering method. One set of samples was tempered for two hours and heat up time at each tempering temperature. Heat up time is dependent on the furnace and the tempering

temperature, this time varied from 15-20 minutes over the four tempering temperatures. Upon the completion of the first heat of double each double-tempering cycle, the samples were removed from the furnace and allowed to cool to room temperature. One of the 10 mm by 12.7 mm ends of each sample polished with 240 grit sandpaper to remove oxidation and process chemicals that remained on the samples from when the samples were cut using water jet cutting and quenched in oil.

Once the samples were polished, a hardness test was conducted using a Rockwell-type hardness tester. After calibration of the machine using 45.9 RC and 62.9 RC test blocks, each of the five samples were hardness tested in five locations, and the readouts were recorded and averaged in an excel sheet. The samples were hardness tested after the first two hours to indicate the effect if the second tempering cycle on the surface hardness of the samples.

Once the samples were polished, a hardness test was conducted using a Rockwell-type hardness tester. After calibration of the machine using 45.9 RC and 62.9 RC test blocks, each of the five samples were hardness tested in five locations, and the readouts were recorded and averaged in an excel sheet. The samples were hardness tested after the first two hours to indicate the effect if the second tempering cycle on the surface hardness of the samples.

Upon completion of surface hardness testing of the first two-hour temper, the samples were then tempered again for another two hours in addition to the heat time at each tempering temperature. The samples were removed upon completion of the second two hours and allowed to air cool to room temperature. The same end that had been polished after the first tempering cycle was polished using 400 grit sandpaper to ensure a similar testing surface for hardness testing. Each sample was surface hardness tested five times and their hardness recorded and averaged in the same excel sheet, and the overall surface hardness average for each tempering temperature the second temper time was calculated.

One set of five samples were tempered for four hours and equivalent heat up times, at each tempering temperature. The samples were allowed to cool to room temperature for a range of 3-4 hours. Once cooled a single 10 mm by 12.5mm ends of the sample was selected and polished using 240 grit sandpaper using a blank polishing machine to again remove the grit and coolant leftover from the waterjet cutting completed to get the rough samples from the original plate. Once polished the samples were hardness tested a Rockwell-type hardness machine. The machine was calibrated each time before a sample set is tested. The samples were surface hardness tested five times, and averaged for each sample, and the final average surface hardness for four hours of tempering at each temperature was calculated.

Before impact testing could be completed, the samples first needed to me milled to the final dimensions of 10 mm by 10 mm by 55 mm listed in the ASTM Standard for Charpy impact testing. The operation was carried out on a Haas Minimill located in Washburn Shops 107. Each sample was measured via micrometer to

confirm that the dimensions established during waterjet cutting were within the tolerances of 10 mm ± 0.075 mm width and 55 mm +0/- 2.5 mm length. The unmachined height dimension, corresponding to the as-manufactured thickness of the original plate, was also measured and consistently found to be to 13.4 mm (0.5275in.), slightly greater than the listed 12.7 mm (0.5 in).

The first attempt to remove the excess material began with the creation of a program using G-code. A simple operation was planned using a half-inch carbide ferrous end mill to remove 3.4 mm of material in a single pass. Using resources available on the MFE Labs website for 4000-series alloy steel in material group P3, an initial cutting speed of 450 surface feet per minute (SFM) and a feed rate of 28.1 inches per minute were selected. Each workpiece was fixtured using a standard CNC vise fitted with 1.75 in. parallels. The tool offset of the end mill was set using an automatic operation, and the work offsets were measured with a precision digital 3-axis probe.

After simulating the code on the Minimill console, a practice sample was loaded into the machine and a dry run of the program was performed by setting the Z-offset to one inch above the sample. The program functioned as intended, and it was decided to move forward with the operation. Immediately upon contact with the workpiece, the endmill broke and the emergency stop button was applied. After investigation of the conditions of the crash, it was determined that the material of the samples had been misclassified, and that due to their high hardness the more appropriate designation was P4 or H1. The depth of cut had been too high, and the power of the spindle was insufficient to drive the endmill through the material, causing it to bind and shatter.

In order to more easily control and modify the parameters of the program, it was recreated in Autodesk Fusion360 software. To compensate for the hardness of the material and the limits of the milling machine, the depth of cut was reduced by a factor of four, a ⅜ inch endmill was selected, and the stepover was increased so that each depth was split into two passes for a total of eight passes. In order to preserve the heat treatment of each sample, coolant was applied during the operation and material was removed only via climb milling.

Another practice sample was then loaded into the machine, after which the process was again confirmed with a console simulation and dry run. The sample was milled successfully; however, it was not within the tolerances specified in the ASTM standard. The Z-offset was adjusted to a distance equal to the amount of dimensional variance, and another practice sample was loaded and milled to within the correct tolerances. The remainder of the samples were then milled and measured with a micrometer to confirm that they were within tolerance.

The last machining step prior to impact testing was to cut V-notches into each sample. This process was first performed using a horizontal milling machine fitted with a 45-degree double-angle slotting blade that had been fabricated in-house. Due to the hardness of the 300 ºC samples, the blade broke before all of the samples

could be notched. A replacement blade was purchased, and the remainder of the samples were cut without issue and evaluated to confirm that they were within the ASTM standard.

Once milled to final ASTM standards the samples were impact tested. An Instron Charpy Impact Tester was used to impact each sample. The impact energy absorbed by each sample was recorded using the software Fracta. The Fracta software required calibration prior to the use of the machine. This process was complete by setting the maximum pendulum angle to zero and the friction to zero before the pendulum has been moved. The pendulum is then raised to the top position and is latched, the maximum latch angle is calculated and the latch engagement button is pressed. Several practice tests were completed after calibration with no samples fixtured in the machine to ensure there the impact tester was calibrated correctly and that no impact energy was being recorded. If the Fracta software and the impact tester were not calibrated correctly, Fracta would read a negative energy absorption on test swings with no samples fixtured in the impact tester. Once calibration was insured, samples were fixtured one at a time into the impact tester. The pendulum was first raised to point where a safety two by four could be put in place to hold the pendulum back and allow safe environment for the insertion of samples into the fixture. Samples were fixtured using a set of tongs that were specially modified to line up with the notches cut in the samples and the fixturing slot in the impact tester. Notches were position on the opposite side of in which the pendulum impacted the sample. After fixturing the pendulum was raised to the maximum angle latch angle and latched in place. The latch engagement button was then pressed to register in Fracta that the pendulum was in the latch position and ready to be released. With confirmation that the latch is in engaged on Fracta, and manual setting of the dial is set to ensure data is recorded if Fracta does not acknowledge the release of the pendulum. Each sample was tested and the impact energy was recorded in Joules. After each fracture the two pieces of each samples were collected and placed in a labeled bag to ensure proper matching of samples pieces and to ensure the fracture surfaces were not altered.

Before carbides were extracted, a training was conducted by PhD student Haixuan Yu. He trained the team on how to use the machines and how to get the samples ready for XRD testing. For the carbide extraction of the samples, an electro polishing machine was used. This iterative process started by cutting a small portion of each impact tested sample. The sample were cut in the direction of the grain. Once a thin section was obtained, it was partially submerged in a solution of 4% hydrochloric acid and ethanol. The electropolishing machine was connected to the solution with the sample and was set to run at a voltage of 120 for approximately 1.5 hours. Once all the carbides were on the surface of the sample, it was removed carefully and placed in a small beaker. Ethanol was added to just cover the sample, and the beaker was placed in an ultrasonic cleaning machine. In this machine, the carbides resting on the surface of the sample transferred to the ethanol. The solution of carbides and ethanol was placed into small capsules using a dropper. The capsule was then placed in a centrifuge in order to separate the carbides from the ethanol/hydrochloric solution. When enough carbides are

extracted, a purification process was conducted in order to eliminate residual hydrochloric acid. During the purification process, ethanol was added into the capsule and re-centrifuged to flush out remaining acid. This process was completed once the liquid solution was visually clear without any yellowish coloration. In order to get the samples ready for XRD testing, the carbides were placed on rectangular testing glass slides. This preparation was accomplished by extracting the majority of ethanol in the capsule and using a dropper to place the carbides on the glass.

Eight samples were selected for fracture surface fractography, this was due to limited availability of the SEM and the project deadline. The samples were chosen based upon their energy absorbed during impact testing. Samples were chosen that best represented the average impact energy from each tempering temperature and tempering method. A single sample was fixtured on a conductive plate with copper tape and inserted into SEM to ensure no two samples were mistaken for another. The fracture surface of each sample was pictured at 200, 500, 1,000, and 2,000 magnifications. Fracture surfaces pictures were taken about the middle of the samples. With the completion of fracture surface fractography, the same eight samples were cut for mounting and polishing. Samples were mounted and then polished using the automated polisher up to 1,200 grits. Samples were then removed and polished by hand up to one micron. With the completion of polishing samples were inserted in SEM for micrography. Each sample was pictured at 5,000, 15,000, and 30,000 magnifications.

With the completion of SEM micrography, each desired property for both tempering methods and each tempering temperature had been observed.

Experimental Results

This section describes the results from each measured and observed property from both tempering methods and each tempering temperature has been observed.

Hardness Testing

Hardness testing was completed on each tempered sample, surface hardness was also measured at each temperature after cooling of the first cycle and prior to the beginning of the second cycle of the double tempering method. This hardness testing was completed to see if the first or second tempering cycle would have a major impact on the final hardness of the samples or if there would be a major difference between the final hardness of the two plus two hours tempered samples. Shown below is the final results from each hardness test completed. Each sample was hardness tested five times, the averages for each sample are shown below in Tables 6-9.

	Sample 1	Sample 2	Sample 3	Sample 4	Sample 5	Average
600 ºC 4hrs Hardness	31.9	32.68	32.52	32.82	31.44	32.272
1st 600 ºC 2hrs Hardness	29.72	30.32	30.18	30.88	30.34	30.288
2nd 600 2hrs Hardness	32.86	32.38	31.8	32.4	31.96	32.28

Table 6: 600 ºC Hardness Averages

	Sample 1	Sample 2	Sample 3	Sample 4	Sample 5	Average
500 ºC 4hrs Hardness	38.64	37.98	37.46	37.58	38.4	38.012
1st 500 ºC 2hrs Hardness	39.58	38.92	39.06	40.22	38.52	39.26
2nd 500 ºC 2hrs Hardness	37.58	36.64	38.04	37.5	36.84	37.32

Table 7: 500 ºC Hardness Averages

	Sample 1	Sample 2	Sample 3	Sample 4	Sample 5	Average
400 ºC 4hrs Hardness	44.2	43.62	45.24	43.28	43.5	43.968
1st 400 ºC 2hrs Hardness	43.74	44.2	42.18	43.8	44.8	43.744
2nd 400 ºC 2hrs Hardness	44.42	44.56	45.08	44.14	43.92	44.424

Table 8: 400 ºC Hardness Averages

	Sample 1	Sample 2	Sample 3	Sample 4	Sample 5	Average
300 ºC 4hrs Hardness	51.04	50.92	51.16	51.62	51.28	51.204
1st 300 ºC 2hrs Hardness	47.34	48.36	47.86	46.84	48.22	47.724
2nd 300 ºC 2hrs Hardness	49.82	51.28	51.04	51.24	50.48	50.772

Table 9: 300 ºC Hardness Averages

There is very little variation in the surface hardness of samples between the two tempering methods. Rockwell hardness is measured with a plus minus of 1 and rounded to the nearest whole number.

Impact testing

Impact testing data was recorded in joules and displayed below. The impact energy absorbed was recorded with the Fracta software and manually using the impact machine's dial. Manual records needed to be kept as Fracta software would not read when the pendulum was not released in some calibration test and in two of the samples tests. If Fracta did not read that the pendulum has been released then the impact energy from that test would not be recorded. The tests in which the impact energy was recorded manually are bolded and underlined in tables 10- 13.

	Sample 1	Sample 2	Sample 3	Sample 4	Sample 5	Average
600 ºC 4hrs	29.33	24.13	29.21	26.25	25.3	26.84
600 ºC 2hrs + 2hrs	28.5	26.96	25.89	26.48	22.85	26.14

Table 10: Impact Energy Absorbed at 600 ºC

	Sample 1	Sample 2	Sample 3	Sample 4	Sample 5	Average
500 ºC 4hrs	16.31	16.54	16.65	15.08	15.19	15.95
500 ºC 2hrs + 2hrs	**13.6**	14.52	15.08	12.84	16.2	14,45

Table 11: Impact Energy Absorbed at 500 ºC

	Sample 1	Sample 2	Sample 3	Sample 4	Sample 5	Average
400 ºC 4hrs	**9.5**	7.81	7.92	**8**	7.27	8.10
400 ºC 2hrs + 2hrs	11.85	12.07	9.76	7.81	14.18	11.13

Table 12: Impact Energy Absorbed at 400 ºC

	Sample 1	Sample 2	Sample 3	Sample 4	Sample 5	Average
300 ºC 4hrs	8.57	8.78	8.57	10.86	8.78	9.11
300 ºC 2hrs + 2hrs	11.08	10.86	10.53	11.85	10.42	10.95

Table 13: Impact Energy Absorbed at 300 ºC

Fracture Surfaces

The fracture surface from one sample from each tempering temperature and a tempering method was observed using SEM. The sample with the closet impact energy to the average from each tempering temperature and tempering method were selected for observation under SEM. There was a wide variation in the 400 ºC two hours + two hours impact energies. The fracture surface from the high and low impact energy samples from the 400 ºC two hours plus two hours were also observed under SEM. Each sample was observed at 200, 500, 1,000, and 2,000 magnifications. The x500 and x1,000 magnification pictures for the average impact energy

sample from each tempering temperature and tempering method are shown below in Figure 9 and 10.

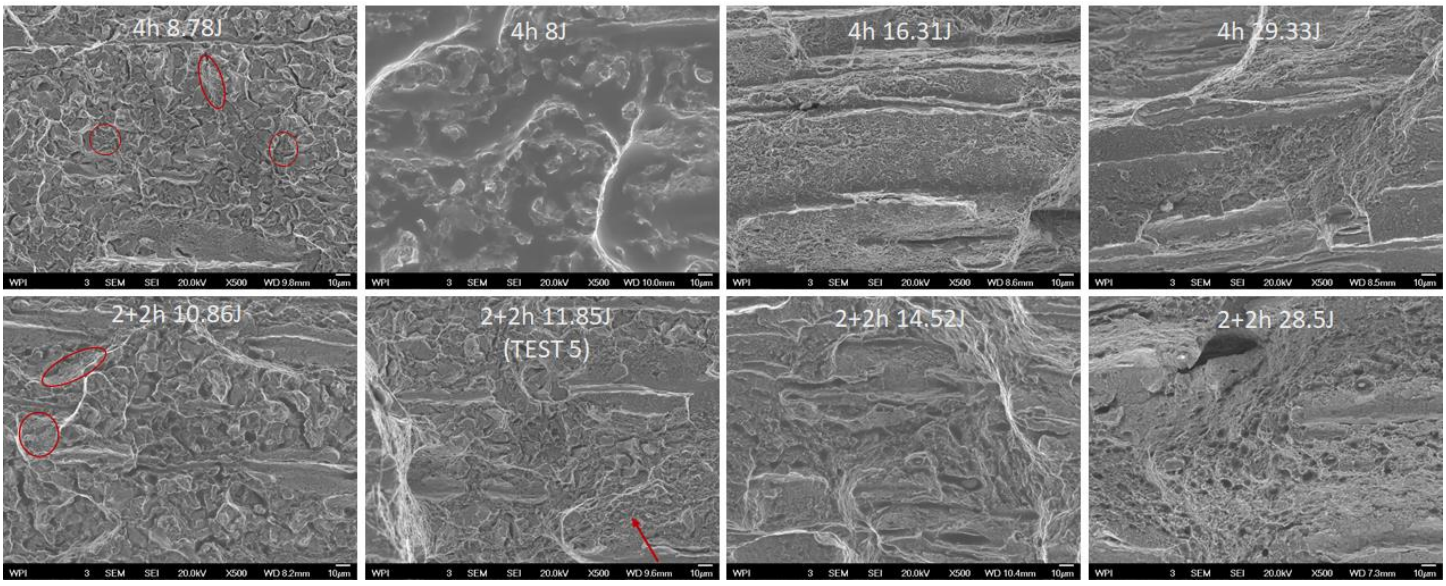

300C
Faceted and grainy texture; Small amount of ductile fracture along cleavage plane

400C
Transgranular fracture; some ductile dimples observed

500C
Ductile fracture with very little transgranular manner

600C
Only ductile fracture; Large dimples observed

Figure 9: Fracture Surface of one sample from each tempering time and temperature at x500 magnification

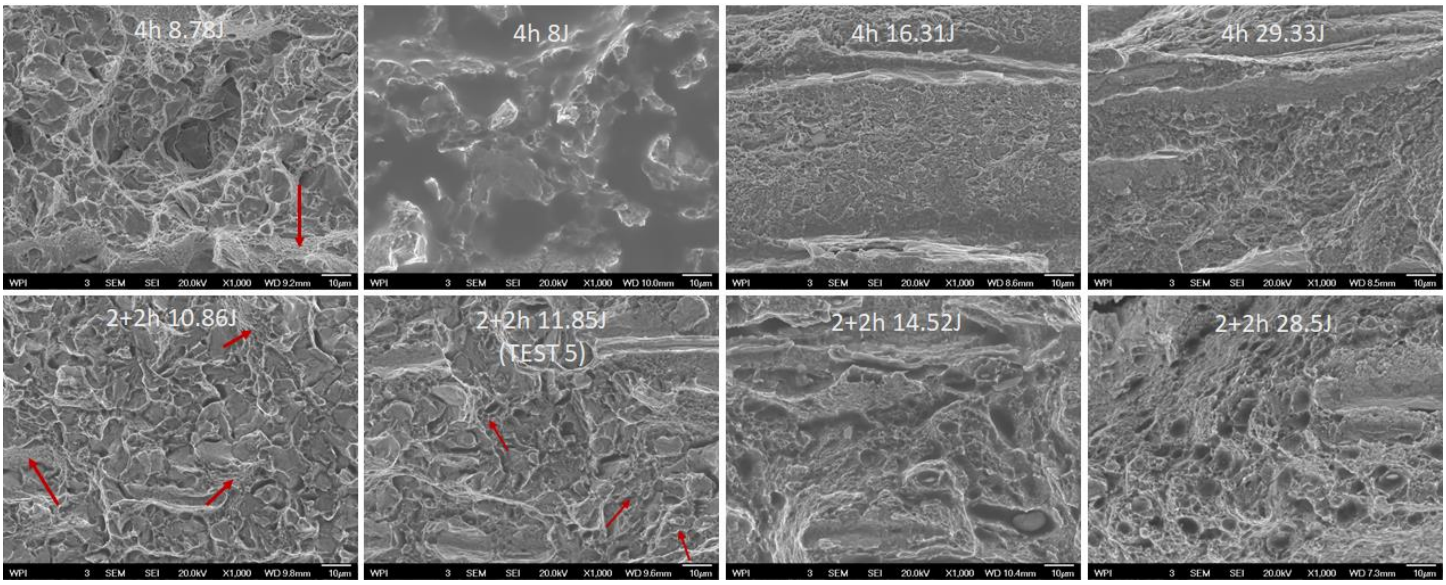

300C
Faceted and grainy texture; Small amount of ductile fracture along cleavage plane

400C
Transgranular fracture; some ductile dimples observed

500C
Ductile fracture; very little transgranular fracture manner

600C
Only ductile fracture; Large dimples observed

Figure 10: Fracture Surface of one sample from each tempering time and temperature at x1,000 magnification

The additional fracture surfaces from the variations in the 400 ºC 2hrs + 2hrs tempering samples can be seen below in Figure 11 and 12.

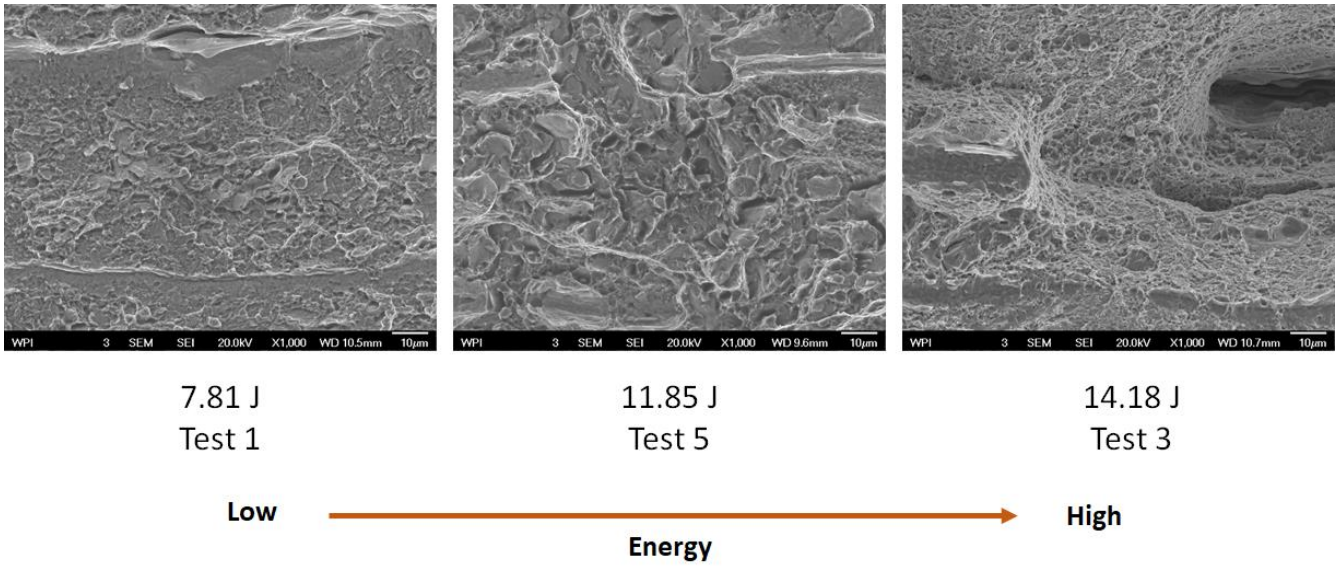

Figure 11: Fracture surface of 400 ºC 2hrs + 2hrs, from low to high energy at x500 magnification

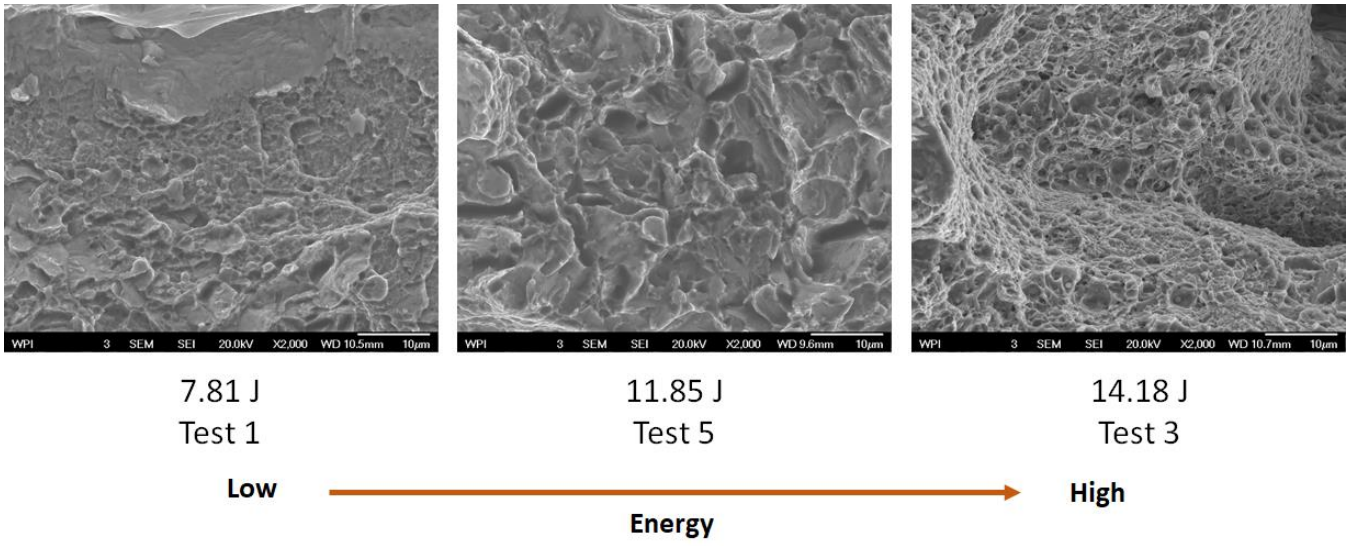

Figure 12: Fracture surface of 400 ºC 2hrs + 2hrs, from low to high energy at x1000 magnification

The average impact energy from the 400 ºC 2hrs + 2hrs tempering set is 11.113 Joules. This average was best represented by test 5, shown in the middle of the fractography displayed above. The lowest absorption in energy, test 1, show a faceted and grainy fracture surface. This fracture surface is comparable to both sets of

the 300 ºC samples, a brittle fracture. The highest impact energy, test 3, displays a dimpled fracture surface. Unlike the fracture surfaces of the 500 ºC tempering samples, who have similar averages for impact energy, but display a transgranular fracture surface. The variation in the fracture surface and impact energy observed in 400 ºC 2hrs + 2hrs sample set could be due to an uneven heating in the furnace during one of the cycles of tempering, placement in the furnace not being uniform when compared to the placement of the other tempering sets, or a microstructural difference in the original martensite composition of each sample in the set prior to tempering.

Carbide Extraction

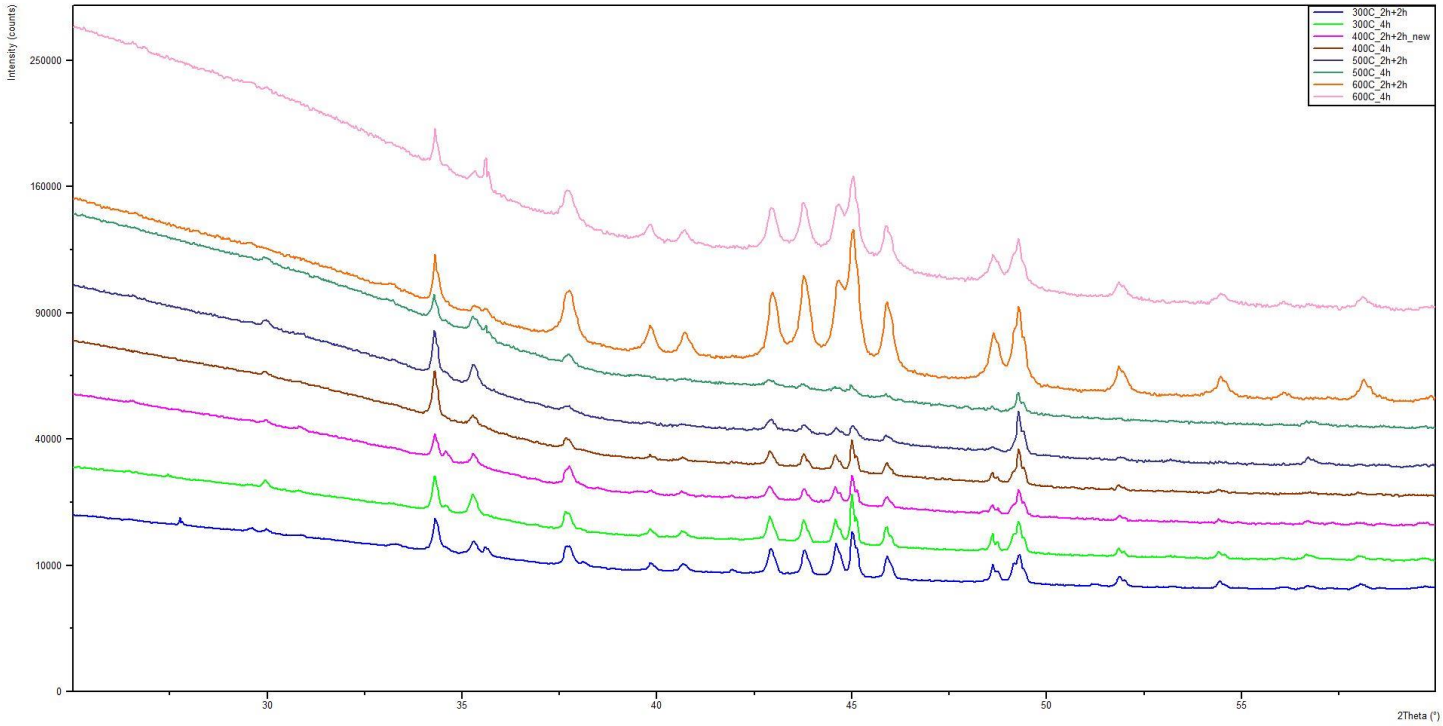

Figure 13: Visual representation of peak size width, and pattern

	300 ºC	400 ºC	500 ºC	600 ºC
Average Carbide Size 4hrs	1715	696	471	470
Average Carbide Size 2hrs + 2hrs	1630	512	512	517

Table 14: Average carbide size from one sample from each tempering temperature and tempering time

By conducting an X-Ray Diffraction test, it was possible to tell which carbides were producing certain peaks, and at what proportion it was increasing or decreasing. From the reading of each peak, it is possible to obtain microstructural information such as carbide size. The results from the micrographs below and sourced literature contradict the results gathered in this investigation. Carbide size should be increasing with tempering

temperatures. Table 14 displays an opposite trend with carbide size decreasing as tempering temperature increases. This extraneous reading might have been an error due to lab procedures, not enough time spent in the electropolishing bath, or mis calibration of the XRD. Only eight samples were tested, one from each tempering temperature and time, due to time restraints. There is no other data from this investigation to compare the results of XRD to. Further extraction of carbides needs to be complete to properly identify the error in this data.

SEM Microstructure

With the completion of carbides extraction, pieces of each of the eight samples with carbides extracted were mounted for SEM polishing. Due to time constraints and SEM availability only eight samples' microstructures were observed using SEM. The samples were pictures using x5,000, x15,000, and x30,000 magnification. The x15,000 and x30,000 magnification pictures from each sample can be seen below in Figure 15 & 16.

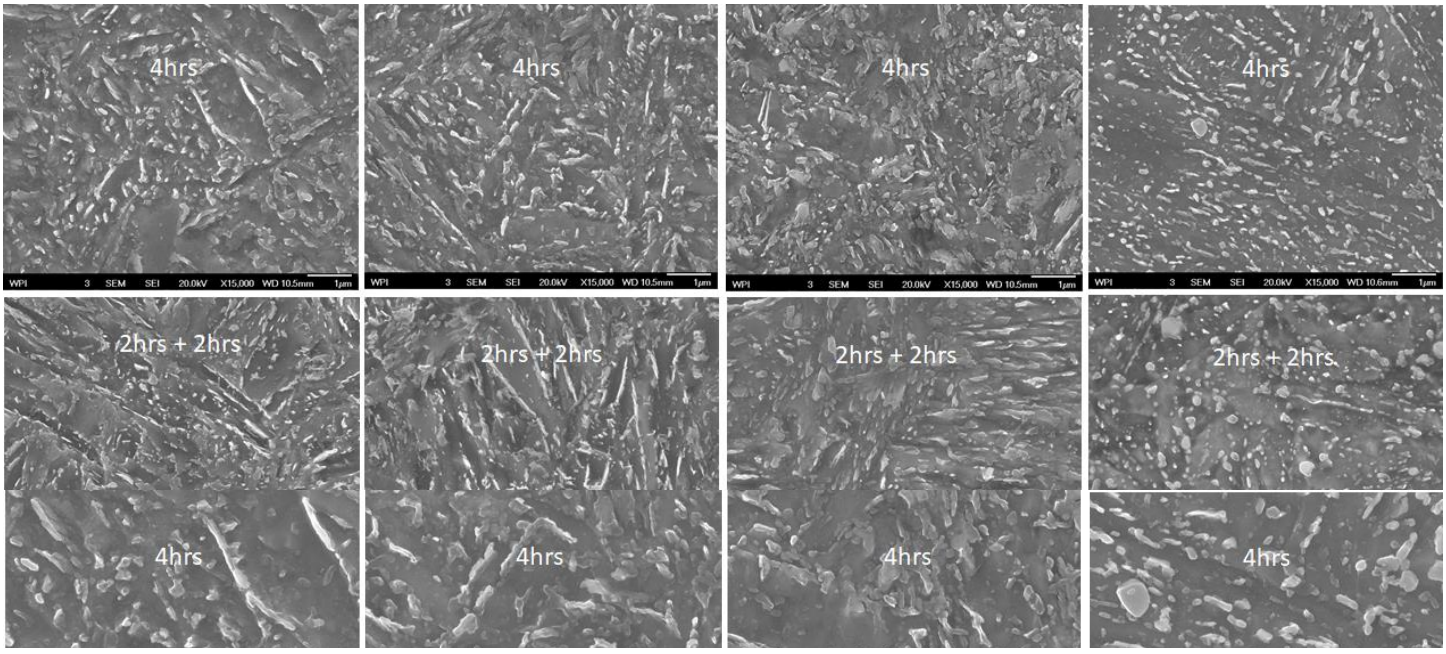

Figure 15: Microstructure of one sample from each tempering time and temperature at x15,000 magnification

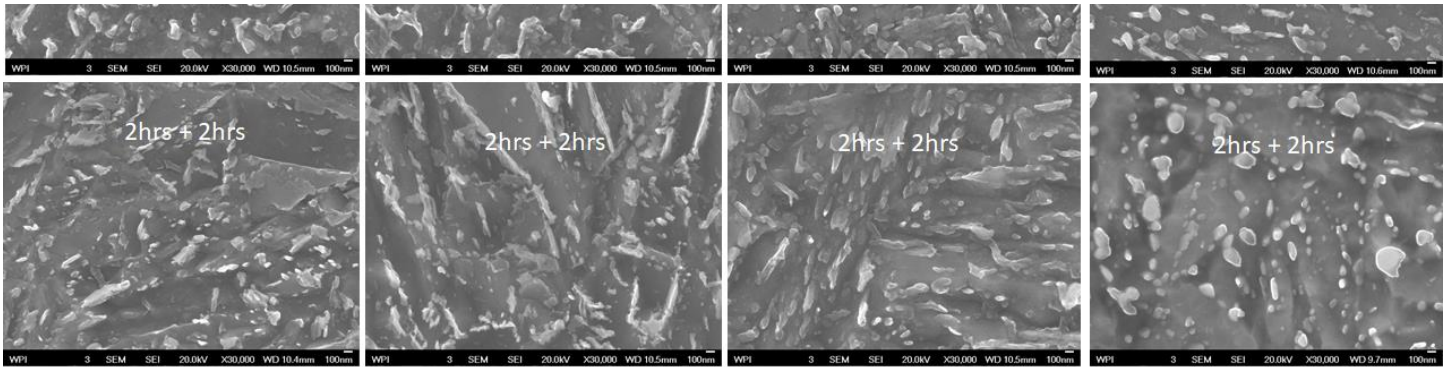

Figure 146: Microstructure of one sample from each tempering time and temperature at x30,000 magnification

Carbides are the bright white coloring seen in the micrography above. They grow within the martensite which is the lighter of two shades of gray, and the ferrite that forms during tempering which is darker shade of grey shown in the micrography above. The carbides transition from small elongated particles to larger rounded particles as the tempering temperature increases from left to right.

Discussion

Upon the completion of testing each parameter outlined in our goal, it was crucial to ensure that the data we had collected for the single four hour tempering cycle was consistent with the existing body of work on 4140 steel. It is best to compare the surface hardness of the samples to the tempering time and temperature using the Hollomon-Jaffe parameter. The Hollomon-Jaffe parameter is a dimensionless quantity that can be used when the tempering time and temperature is known to predict the hardness of the alloy. The parameter has been developed for the heat treatment of steel alloys, each alloy has its own derivation and specific C constant parameter range. Figure 17 shows the comparison of the expected hardness line based off the Hollomon-Jaffe parameter and the recorded surface hardness of the samples.

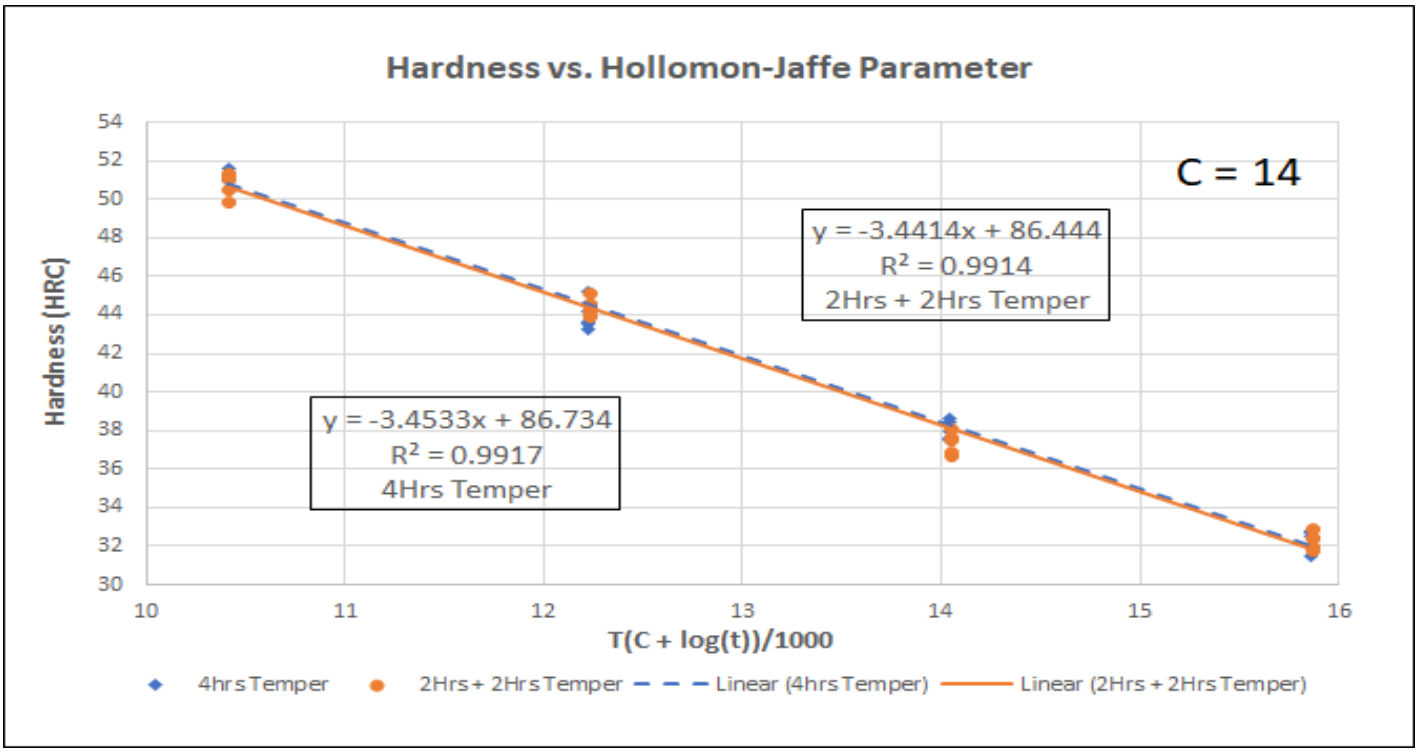

Figure 15: Average surface hardness form each sample vs the Hollomon-Jaffe Parameter

The hardness of the two hours plus two hours tempering cycles have also been plotted on the hardness vs. Hollomon-Jaffe Parameter graph. Temperature increases from left to right as hardness decreases. Each set of data points from both tempering times align with the Hollomon-Jaffe prediction line. The prediction line is different for the two tempering methods due to the difference in time effective between the two tempering methods. The time effective refers to the total time the samples are tempered. Each tempering cycle requires a heat up time, this is the time required for the furnace to climb back to the tempering temperature after the samples have been inserted into the furnace. The time effective is longer for the 2hrs + 2hrs due to the two heat up times that are added together to the total tempering time, making the total time effective for tempering at 2hrs + 2hrs longer then tempering for 4 hours.

Impact energy as a function of tempering temperature is also a well-documented parameter. Impact energy, or energy needed to fracture the sample, will increase as temperature increases. The increase in impact energy is not a linear increase in 4140 steel. This is due to the temper embrittlement temperature range that can affect alloy steels, including 4140. The temper temperature embrittlement range and time at which temper embrittlement effects steels is a debated range in the heat treatment industry. The range for temperature embrittlement is a subject of debated has been reported in the ranges of 250 – 400 ºC (Herring, D. H, 2011), 350- 450 ºC in (Herring, D. H, 2006) and 300- 425 ºC in (Horn, R. M., & Ritchie, R. O. 1978)

The impact energy for both tempering methods as a function of time are plotted below in Figure 18.

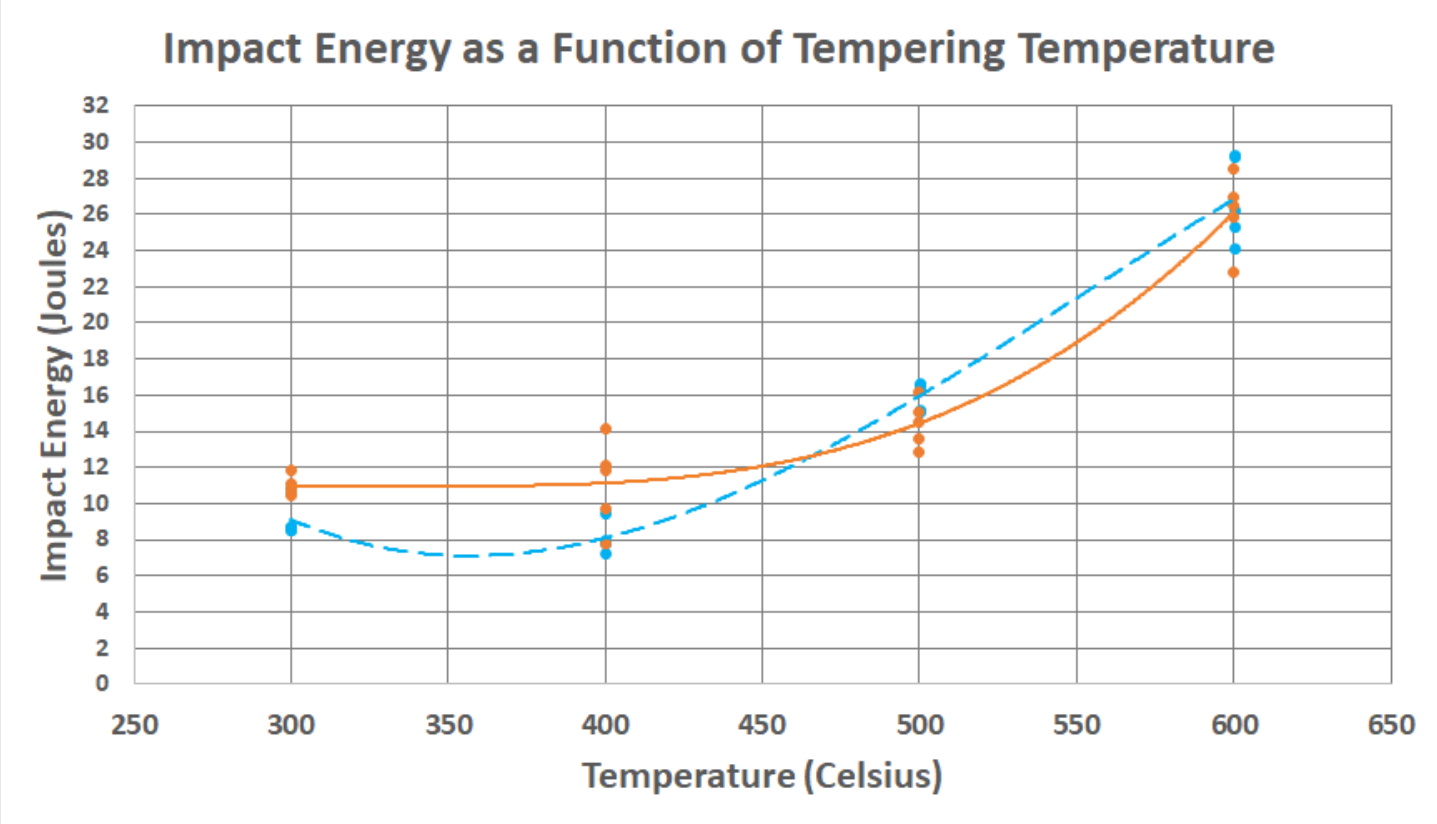

Figure 168: Average impact energy absorbed of each sample as a function of tempering time.

There is some variation in the impact energy of samples tempered at 400 ºC, which causes a slight knee in the line of best fit. As discussed before there are a several factors that could have caused the variation seen in the impact energy of the 400 ºC 2hrs + 2hrs samples. Due to only tempering five samples at each temperature for each tempering method, it is not analytically correct to eliminate outliers or support that there should be variations seen in the impact energy absorbed by the 400 ºC 2hrs + 2hrs.

To begin comparing if there is any difference between the two tempering methods, two plots can be produced to determine if there is a significant difference in the hardness and impact energy absorbed. Figure 19 plots impact energy absorbed and hardness as a function of time, which are correlated when graphed as a function of time; of each sample from each tempering method.

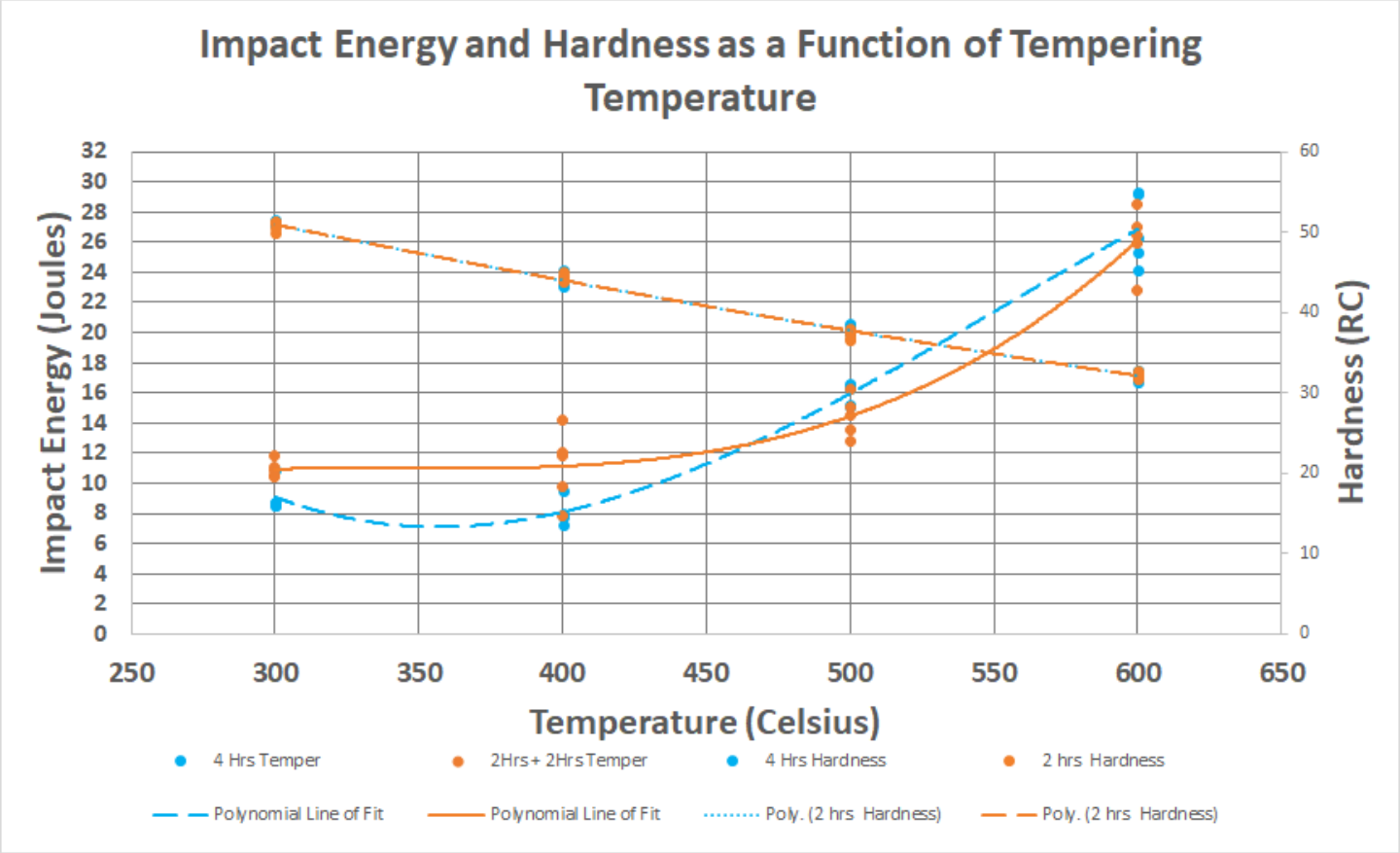

Figure 17: Average impact energy and surface hardness of each sample as a function of tempering temperature. impact energy decreases with increasing temperature

As shown in Figure 19, the surface hardness of 4140 steel decreases with increasing tempering temperatures, while impact energy absorbed increases as tempering temperatures increases. There is no significant variation between the two properties that are plotted above and the two tempering methods. Surface

Hardness vs Impact energy has also been plotted in Figure 20 to compare the two tempering methods and determine if there is any variation.

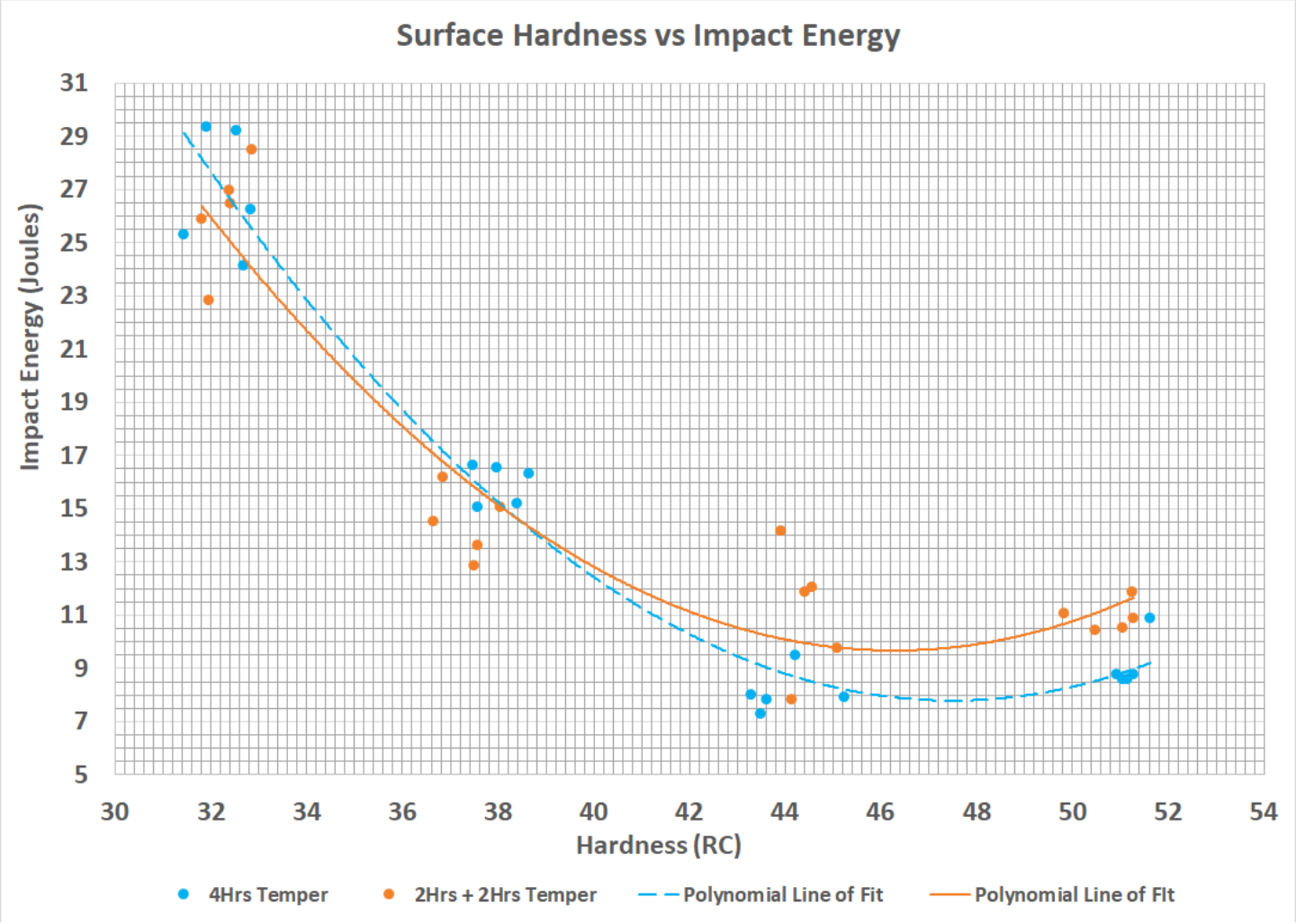

Figure 18: Comparison of surface energy vs impact energy between the two tempering methods

As shown in Figure 17 and Figure 20 there is no significant variation in the recorded surface hardness and impact energy absorbed at each temperature for the two tempering method. Double tempering 4140 steel for four hours vs single tempering 4140 steel for four hours, has no impact on the surface hardness and impact energy of 4140 steel.

Both tempering time's lines of best fit for hardness and impact energy match expected impact energy as function of tempering temperatures from previous sourced literature. An expect plot can be seen below in Figure 21, and when compared to Figure 19 it can be determined that tempering was completed correctly for the single four hour tempering cycle samples

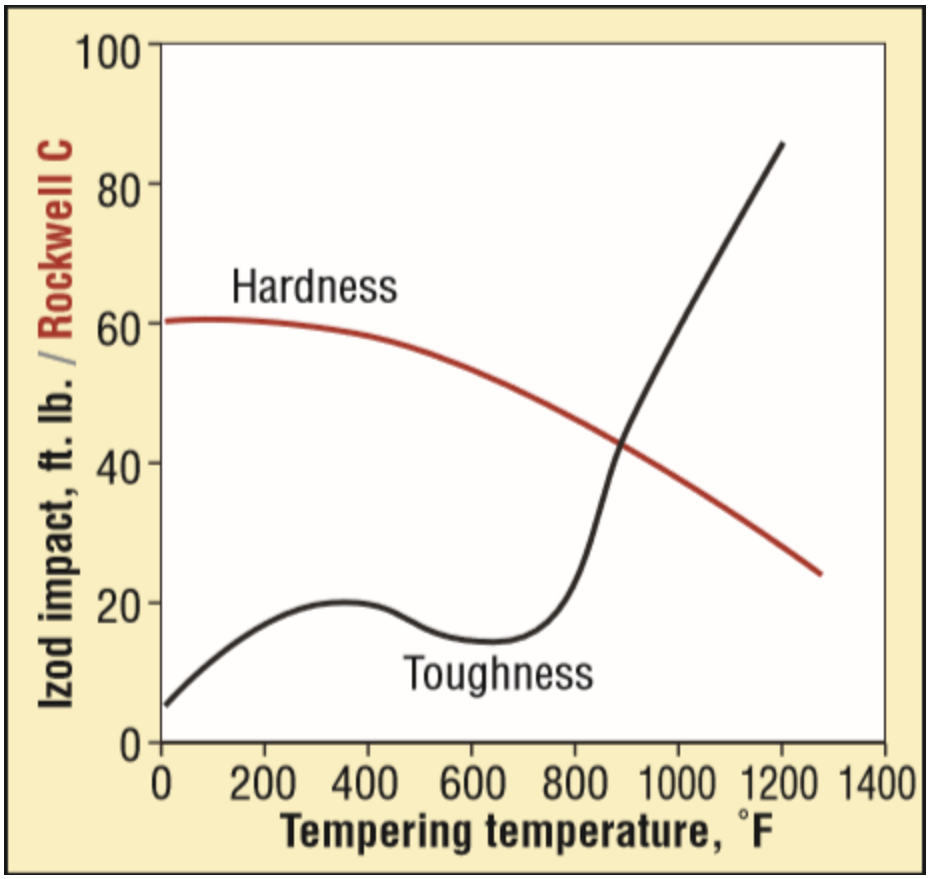

Figure 2119: Impact energy and Rockwell hardness as tempering temperature increases. Herring, D. H. (2011)

Fracture surface was inspected using SEM to investigate the effects of double tempering and to validate the impact energy absorption data recorded during impact testing. If when looking at the fracture surfaces a ductile failure was observed in sample that recorded an impact energy that is correlated with a brittle failure then there would be argument that double tempering can have effect on 4140 steels. In this investigation, no such fracture surfaces were found. As shown in Figure 14 and Figure 15 the fracture surfaces from both tempering method transition from brittle fracture to ductile fracture as tempering temperature increases. Brittle fracture requires minimum impact energy to be absorbed, while ductile fracture require double to triple the amount of absorbed impact energy. This agrees with the data presented in Tables 6-9 and impact energy as function of temperature represented in Figure 18, which show impact energy increasing with temperature. It is expected, that impact energy should increase with tempering temperature and the fracture surface should transition from brittle to ductile with increasing tempering temperature (G.Krauss). The variation seen in the

400 ºC 2hrs + 2hrs samples, do not conform to this pattern described above, there is a large variation within the sample set in fracture surfaces and impact energy which is shown in Figures 11 & 12 and Table 12. A large sample size is needed and further tests into tempering at 400 ºC for a 2hrs + 2hrs tempering cycle to determine if the results from this investigation are outliers or if there were other factors that caused our resulted to be as varied as they were.

Carbides were extracted and measured, and the microstructure of the samples were observed to validate that the single four hours tempering samples had been tempered correctly and to compare the two tempering methods. Carbides are expected to grow in size and transition from elongated cylinders to rounded spheres in the martensite matrix (G. Krauss). This transition was observed in the double tempering cycle samples, as tempering temperature increased.

Conclusion

Based upon the data collected from surface hardness testing, Charpy impact testing, XRD carbide analysis, and SEM microstructure/fracture surface analysis, it was concluded that there is no significant difference between the effects of a single four hour tempering cycle and two two hour tempering cycles, with regards to surface hardness, impact energy, and microstructure, in AISI 4140 steel.

As the tempering temperatures increased, the surface hardness in each sample set decreased. The average Rockwell C hardness for 300 ºC for 4 hours was 51.2 RC, whereas the average Rockwell C hardness for 600 ºC for 4 hrs was 32.3 RC. This is consistent with calculations done using the Hollomon-Jaffe parameter equation. However, the impact energy absorbed rose when the tempering temperatures increased. At 300 ºC, 4 hours tempering, the average impact energy absorbed was 9.11 J and the 600 ºC for 4 hours samples, the average impact energy absorbed was 26.84 J.

When comparing the data collected from the XRD carbide extraction and the SEM fracture surface, there is a distinct inconsistency in carbide size. The SEM fracture surface pictures show an expected increase in carbide size with rising tempering temperature. However, when the carbides were observed using XRD testing, there was a significant decrease in carbide size as the tempering temperature increased. This mismatch in expected results may be due to inconsistent procedure execution, XRD calibration issues or not enough time for each sample in the electropolisher. Testing more samples on both the SEM and XRD could help clarify and correct the inconsistencies found in carbide size.

Future work may include further testing done with tool steel to find a possible difference in the properties investigated in this project. Changing the quenching time and temperature could also cause a difference in properties between a double and single tempering.

Sources

ASTM E23-16b Standard Test Methods for Notched Bar Impact Testing of Metallic Materials, ASTM International, West Conshohocken, PA, 2016, https://doi.org/10.1520/E0023-16B

ASTM A1058-14 Standard Test Methods for Mechanical Testing of Steel Products—Metric, ASTM International, West Conshohocken, PA, 2014, https://doi.org/10.1520/A1058-14

Bhadeshia, H. K. D. H., & Edmonds, D. V. (1979). tempered martensite embrittlement: Role of retained austenite and cementite. *Met Sci, 13*(6), 325-334.

Herring, D. H. (2006). *The embrittlement phenomena in hardened & tempered steel*. Troy: BNP Media\

Herring, D. H. (2011). *Toughness revisited*. Troy: BNP Media.

Horn, R. M., & Ritchie, R. O. (1978). Mechanisms of tempered martensite embrittlement in low alloy steels. Metallurgical Transactions A,9(8), 1039-1053. doi:10.1007/bf02652

Hollomon, J. H. and Jaffe, L. D. 1945. Time-temperature Relations in Tempering Steel. New York Meeting

Krauss, George, 2005. *Steels: Processing, structure, and performance*. 2005th ed. Materials Park, Ohio: ASM International.

Krauss, G. (1999). Martensite in steel: Strength and structure. *Materials Science and Engineering a-Structural Materials Properties Microstructure and Processing, 275*, 40-57

Moeck, P., PhD. 2004, X-ray Diffraction (XRD). Retrieved from http://web.pdx.edu/~pmoeck/phy381/Topic5a-XRD.pdf

Siewert, T. A., Manahan, M. P., McCowan, C. N., Holt, J. M., Marsh, F. J. and Ruth, E. A., "The History and Importance of Impact Testing," Pendulum Impact Testing: A Century of Progress, ASTM STP 1380, T. A. Siewert and M. P. Manahan, Sr., Eds., American Society for Testing and Materials, West Conshohocken, PA, 1999.

Swapp, S. (2017, May 26). Scanning Electron Microscopy (SEM). Retrieved from http://www2.lbl.gov/ritchie/Library/PDF/1978_Horn_MetTransA_MechanismsOfTemperedMartensite.pdf

Appendix A

600 ºC 4hrs Surface Hardness

	Sample 1	Sample 2	Sample 3	Sample 4	Sample 5
Trial 1	30.9	33.8	32.9	32.9	31.9
Trial 2	32.9	33.9	32.9	33	33
Trial 3	32	32.1	32.2	32	30.8
Trial 4	33.3	32.4	32	33.1	30.8
Trial 5	30.4	31.2	32.6	33.1	30.7
Averages	31.9	32.68	32.52	32.82	31.44

600 ºC 2hrs + 2hrs Surface Hardness

1st cycle

	Sample 1	Sample 2	Sample 3	Sample 4	Sample 5
Trial 1	29.4	31	29	32.3	30.1
Trial 2	30.1	30.8	30.9	31.8	31.4
Trial 3	30.8	29.6	28.2	31	30.9
Trial 4	29.3	30	31.6	30.5	30.1
Trial 5	29	30.2	31.2	28.8	29.2
Averages	29.72	30.32	30.18	30.88	30.34

2nd cycle

	Sample 1	Sample 2	Sample 3	Sample 4	Sample 5
Trial 1	33.1	32	31	32	32
Trial 2	32.4	32.9	33	34	31.6
Trial 3	33.6	31.5	30.5	32.5	32.7
Trial 4	32.7	33	33.5	32	32.5
Trial 5	32.5	32.5	31	31.5	31
Averages	32.86	32.38	31.8	32.4	31.96

500 ºC 4hrs Surface Hardness

	Sample 1	Sample 2	Sample 3	Sample 4	Sample 5
Trial 1	37.8	37.9	36	36	40.1
Trial 2	38.1	38.5	37.2	37	38
Trial 3	37.9	36.3	35.1	37.6	37.9
Trial 4	39.9	38.3	39.5	38.1	38.9
Trial 5	39.5	38.9	39.5	39.2	37.1
Averages	38.64	37.98	37.46	37.58	38.4

500 ºC 2hrs + 2hrs Surface Hardness

1st cycle

	Sample 1	Sample 2	Sample 3	Sample 4	Sample 5
Trial 1	39.5	38.3	38.2	39.6	39.4
Trial 2	39.6	39.2	38.9	40.7	37.1
Trial 3	39.5	38.5	39.3	40.9	38.5
Trial 4	39.4	39.5	39.5	39.4	37.9
Trial 5	39.9	39.1	39.4	40.5	39.7
Averages	39.58	38.92	39.06	40.22	38.52

2nd cycle

	Sample 1	Sample 2	Sample 3	Sample 4	Sample 5
Trial 1	37.3	36	36.9	37.3	35
Trial 2	37.8	38.2	38	37	36.1
Trial 3	38.6	37.2	38.8	37.9	36.3
Trial 4	37.4	36.3	37.5	37	37.8
Trial 5	36.8	35.5	39	38.3	39
Averages	37.58	36.64	38.04	37.5	36.84

400 ºC 4hrs Surface Hardness

	Sample 1	Sample 2	Sample 3	Sample 4	Sample 5
Trial 1 (RC)	40.4	40.7	44.3	43.1	39.9
Trial 2 (RC)	42.2	44.1	42.5	45	44.9
Trial 3 (RC)	44.5	46.2	46.5	40.9	43.9
Trial 4 (RC)	46.9	45	47	45.5	43.8
Trial 5 (RC)	47	42.1	45.9	41.9	45
Average	44.2	43.62	45.24	43.28	43.5

400 ºC 2hrs + 2hrs Surface Hardness

1st cycle

	Sample 1	Sample 2	Sample 3	Sample 4	Sample 5
Trial 1	40	43.3	38	43.4	42.5
Trial 2	43.8	40	43.9	44.7	46.1
Trial 3	43.8	46	44	43.8	45.3
Trial 4	45	45.7	40.8	42.3	44.5
Trial 5	46.1	46	44.2	44.8	45.6
Averages	43.74	44.2	42.18	43.8	44.8

2nd cycle

	Sample 1	Sample 2	Sample 3	Sample 4	Sample 5
Trial 1	42	46	46	43.2	44.5
Trial 2	44.8	42.8	45	45.6	45
Trial 3	45.2	44.6	46.2	43.3	44.9
Trial 4	44.7	44.4	44.2	44.5	42.3
Trial 5	45.4	45	44	44.1	42.9
Averages	44.42	44.56	45.08	44.14	43.92

300 ºC 4hrs Surface Hardness

	Sample 1	Sample 2	Sample 3	Sample 4	Sample 5
Trial 1	52.1	52.1	51.9	51.9	52.1
Trial 2	50.1	52.1	50.6	52.1	51.9
Trial 3	50.2	49.9	51.1	51.8	49
Trial 4	50.9	50	50.2	50.2	51.8
Trial 5	51.9	50.5	52	52.1	51.6
Averages	51.04	50.92	51.16	51.62	51.28

300 ºC 2hrs + 2hrs Surface Hardness

1st cycle

	Sample 1	Sample 2	Sample 3	Sample 4	Sample 5
Trial 1	45.1	49.1	48.3	47.2	49.8
Trial 2	48.1	47	49.7	48.1	49
Trial 3	47.6	48.5	47.2	47	46.2
Trial 4	48.1	49.2	46	45.8	47.1
Trial 5	47.8	48	48.1	46.1	49
Averages	47.34	48.36	47.86	46.84	48.22

2nd cycle

	Sample 1	Sample 2	Sample 3	Sample 4	Sample 5
Trial 1	48.4	50.9	53	52	49.8
Trial 2	49.3	52	50	50.9	51.6
Trial 3	50.2	51.3	51	50.8	50.3
Trial 4	50.2	50.2	50.9	51.2	50.2
Trial 5	51	52	50.3	51.3	50.5
Averages	49.82	51.28	51.04	51.24	50.48

Appendix B

x200 Magnification

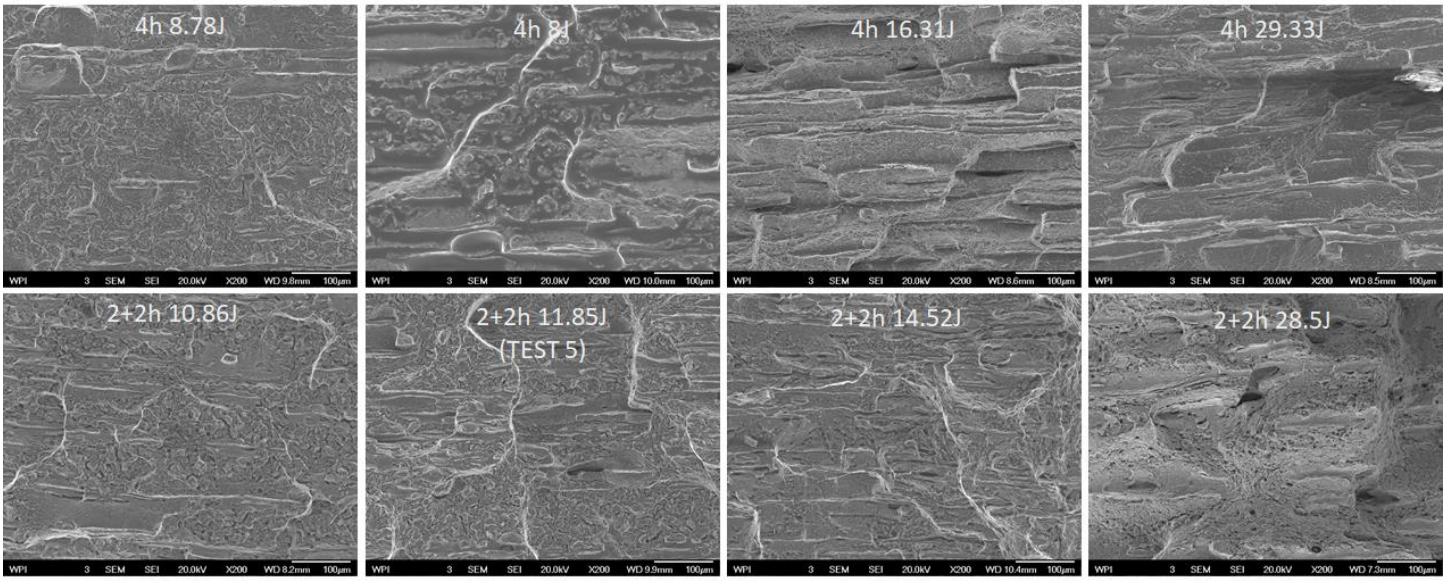

300 °C 400 °C 500 °C 600 °C

x500 Magnification

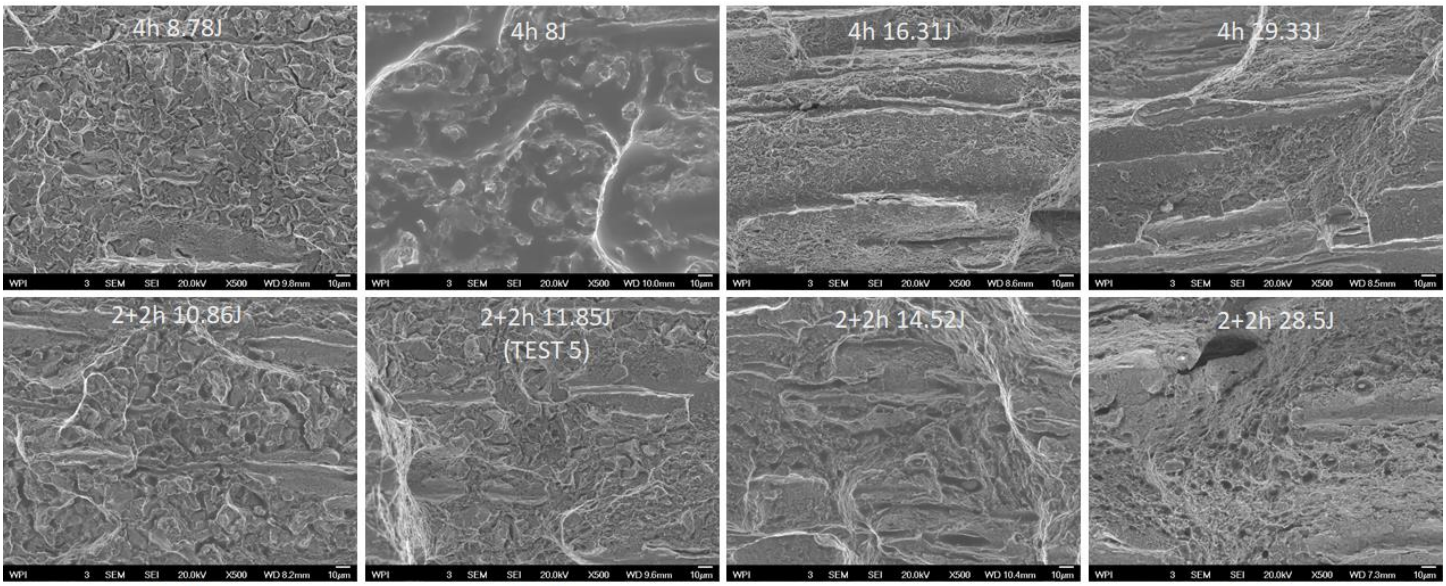

300 °C 400 °C 500 °C 600 °C

x1000 Magnification

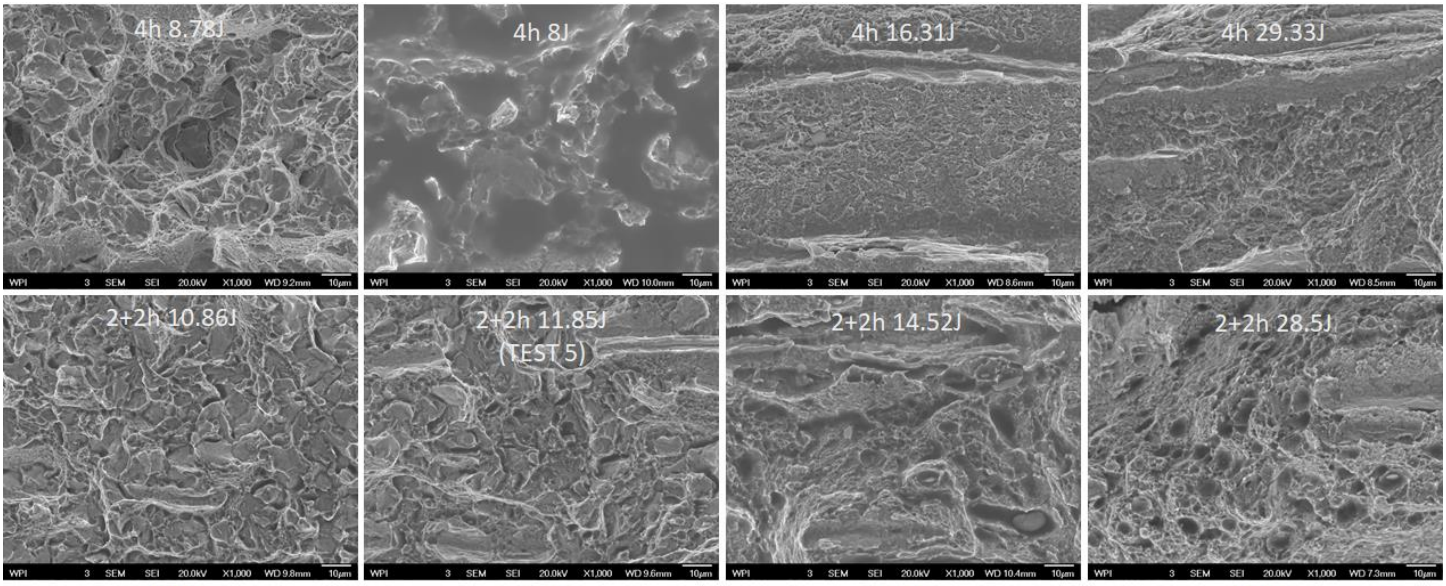

300 °C 400 °C 500 °C 600 °C

x2000 Magnification

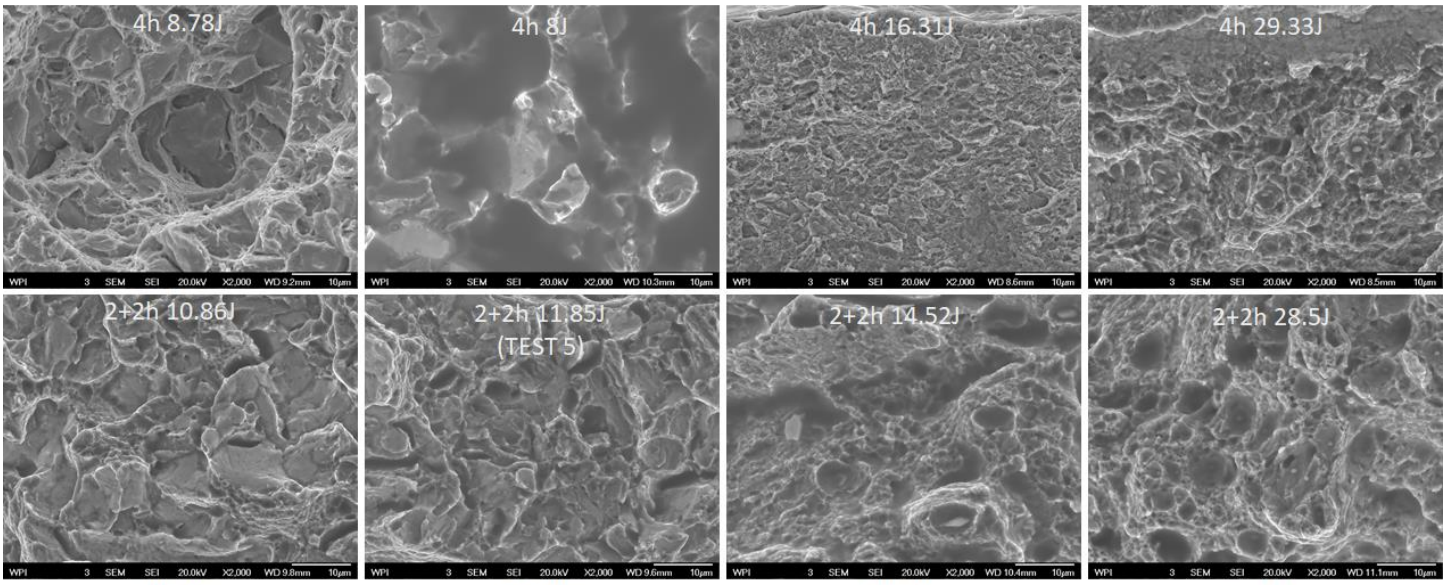

300 °C 400 °C 500 °C 600 °C

400 ºC 2hrs + 2hrs x200 Magnification

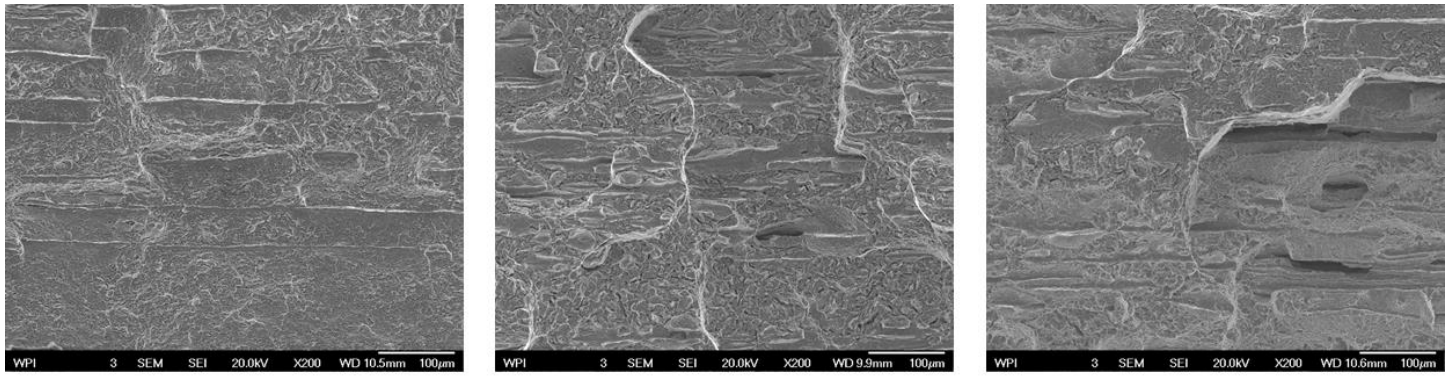

7.81 J
Test 1

11.85 J
Test 5

14.18 J
Test 3

Low → **High**

Energy

400 ºC 2hrs + 2hrs x500 Magnification

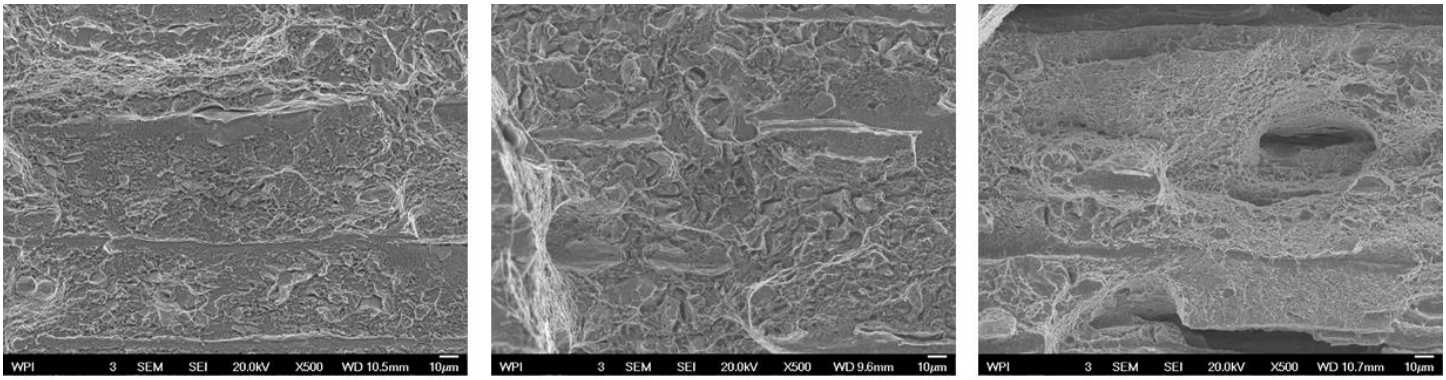

7.81 J
Test 1

11.85 J
Test 5

14.18 J
Test 3

Low → **High**

Energy